Article

# A Rigorous Framework To Interpret Water Relaxivity. The Case Study of a Gd(III) Complex with an #-Cyclodextrin Derivative

Ce#lia S. Bonnet, Pascal H. Fries, Andre#e Gadelle, Serge Gambarelli, and Pascale Delangle

*J. Am. Chem. Soc.*, **2008**, 130 (31), 10401-10413 • DOI: 10.1021/ja802347r • Publication Date (Web): 12 July 2008



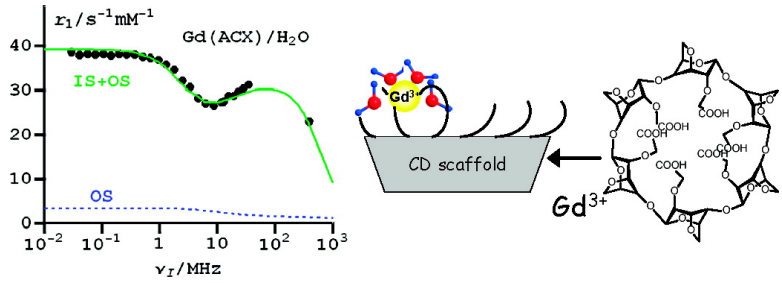


## More About This Article

Additional resources and features associated with this article are available within the HTML version:

- Supporting Information
- Access to high resolution figures
- Links to articles and content related to this article
- Copyright permission to reproduce figures and/or text from this article

View the Full Text HTML

J|A|C|S
ARTICLES

Published on Web 07/12/2008

# A Rigorous Framework To Interpret Water Relaxivity. The Case Study of a Gd(III) Complex with an α-Cyclodextrin Derivative

Célia S. Bonnet,[†,§] Pascal H. Fries,*[,†] Andrée Gadelle,[†] Serge Gambarelli,[‡] and Pascale Delangle*[,†]

*Laboratoire de Reconnaissance Ionique et de Chimie de Coordination and Laboratoire de Résonance Magnétique, INAC/SCIB (UMR_E 3 CEA-UJF), CEA-Grenoble, 17 rue des Martyrs, F-38054 Grenoble Cedex 9, France*

Received April 3, 2008; E-mail: pascale.delangle@cea.fr; pascal-h.fries@cea.fr

***Abstract:*** We present a general theoretical framework suitable for an economical, but rigorous, analysis of the relaxivity and EPR data of paramagnetic metal complexes. This framework is based on the so-called Grenoble method that properly accounts for the fluctuations of the "static" zero-field splitting Hamiltonian and avoids the misinterpretation of experimental data, which occurs with the Solomon, Bloembergen, and Morgan (SBM) formalism and may lead to erroneous conclusions. The applicability of the SBM approximation is discussed. Our approach is implemented in the case of a new $Gd^{3+}$ chelate with a cyclodextrin derivative ligand hexakis(2-*O*-carboxymethyl-3,6-anhydro)-α-cyclodextrin (ACX), designed to obtain lanthanide complexes of enhanced stability in comparison to natural cyclodextrins. The introduction of carboxymethyl units on the six residual hydroxyl groups of an α-*per*-3,6-anhydro cyclodextrin leads to mono- and binuclear $Ln^{3+}$ complexes with $\log \beta_{110} \approx 7.5$. The GdACX complex induces large water proton relaxivity in 0.1 M KCl aqueous solution. The molecular parameters governing the longitudinal ($r_1$) and transverse ($r_2$) relaxivities above 1 T are obtained through simple SBM-like theoretical expressions and complementary experimental techniques. The metal hydration state, the translational diffusion coefficient of the complex, and its rotational correlation time are derived from luminescence lifetime studies, pulse-field gradient NMR, and deuteron quadrupolar relaxation, respectively. The high relaxivity induced by the GdACX complex is attributed to its high hydration state in the presence of potassium ions and to a rotational correlation time lengthened by the hydrophilic character of the ACX scaffold.

## 1. Introduction

Magnetic resonance imaging (MRI) has become a routine diagnostic tool because it is noninvasive and has submillimeter spatial resolution.[1–4] In order to increase the image contrast of the observed nuclear spins of the water hydrogen atoms, paramagnetic $Gd^{3+}$ complexes are injected to the patients in more than 10 million MRI examinations per year. This explains the two-decade race to prepare $Gd^{3+}$-based contrast agents (CAs) having the highest possible efficiency, named relaxivity. Since the early days of MRI, the standard strategy to improve relaxivity has been based on the synthesis of stable $Gd^{3+}$ complexes with molecular properties tailored to yield the maximal value of the Solomon−Bloembergen−Morgan (SBM) inner-sphere (IS) contribution to the relaxivity, which stems from the metal-bound water in continuous exchange with bulk water.[1–6] In particular, nuclear magnetic relaxation dispersion (NMRD) profiles, i.e., the relaxivity values vs magnetic field, and electronic paramagnetic resonance (EPR) spectra have been measured and interpreted to derive molecular parameters affecting the relaxivity and check their optimization with respect to the SBM-IS expression. However, through the careful analysis of EPR spectra of $Gd^{3+}$ complexes, it was realized that in a molecular (M) frame rigidly bound to the complex, the zero-field splitting (ZFS) Hamiltonian acting on $Gd^{3+}$ has a significant time-averaged static value.[7–9] The presence of this static ZFS contribution questioned the popular SBM formalism and was the starting point of renewed theoretical efforts toward a proper theory of electronic spin relaxation and relaxivity of

[†] Laboratoire de Reconnaissance Ionique et de Chimie de Coordination.
[‡] Laboratoire de Résonance Magnétique.
[§] Present address: School of Chemistry, Centre for Synthesis and Chemical Biology, Trinity College Dublin, Dublin 2, Ireland.

(1) Caravan, P. *Chem. Soc. Rev.* **2006**, *35*, 512–523.
(2) Caravan, P.; Ellison, J. J.; McMurry, T. J.; Lauffer, R. B. *Chem. Rev.* **1999**, *99*, 2293–2352.
(3) Merbach, A. E.; Toth, E., *The Chemistry of Contrast Agents*; Wiley: New York, 2001.
(4) Aime, S.; Botta, M.; Terreno, E. *Adv. Inorg. Chem.* **2005**, *57*, 173–237.
(5) Caravan, P.; Cloutier, N. J.; Greenfield, M. T.; McDermid, S. A.; Dunham, S. U.; Bulte, J. W. M.; Amedio, J. C.; Looby, R. J.; Supkowski, R. M.; Horrocks, W. D.; McMurry, T. J.; Lauffer, R. B. *J. Am. Chem. Soc.* **2002**, *124*, 3152–3162.
(6) Vander Elst, L.; Port, M.; Raynal, I.; Simonot, C.; Muller, R. N. *Eur. J. Inorg. Chem.* **2003**, 2495–2501.
(7) Rast, S.; Fries, P. H.; Belorizky, E. *J. Chim. Phys.* **1999**, *96*, 1543–1550.
(8) Rast, S.; Fries, P. H.; Belorizky, E. *J. Chem. Phys.* **2000**, *113*, 8724–8735.
(9) Rast, S.; Borel, A.; Helm, L.; Belorizky, E.; Fries, P. H.; Merbach, A. E. *J. Am. Chem. Soc.* **2001**, *123*, 2637–2644.

10.1021/ja802347r CCC: $40.75 

paramagnetic metal ions.[10–14] The theoretical methods developed in Sweden, Grenoble, and Ann Arbor to calculate the IS relaxivity were recently compared for a large number of realistic model systems of complexed metal ions, and the accuracy of the Grenoble method was found to be very satisfactory.[15] Here, we present a general framework using the Grenoble approach and suitable for a rigorous analysis of the relaxivity and EPR data of $Gd^{3+}$, $Mn^{2+}$, and $Fe^{3+}$ complexes. An efficient and proper way to determine the relaxivity molecular factors of a new paramagnetic metal complex is illustrated on a $Gd^{3+}$ chelate with a cyclodextrine derivative. The failure of the SBM approximation, but also its surprising reasonable predictive success at the imaging field values and above, is discussed.

Cyclodextrins (CDs) are cyclic oligosaccharides composed of six, seven, or eight α-1,4-D-glucopyranosyl units and are, respectively, named α-, β-, or γ-CDs. They are formed by the action of certain enzymes on starch and can be described as a shallow truncated cone providing a hydrophobic cavity and a hydrophilic exterior. Due to these properties, they have been extensively used to transport or encapsulate organic compounds at industrial level in area such as medicine, cosmetics, or detergents.[16] The three types of hydroxyl groups (two secondary and one primary) exhibit different reactivities which facilitates the preparation of a range of derivatives. To benefit from a direct interaction of the $Ln^{3+}$ ion with the CD scaffold, we are developing CD derivatives which are functionalized with $Ln^{3+}$ coordinating groups. The direct interaction of $Ln^{3+}$ with the CD itself is barely reported because the hydrophobic cavity of this ligand is not suited for cations.[17,18] The chemical modification of native CDs, leading to *per*-3,6-anhydro derivatives,[19,20] drastically affects the structure of the CD host giving rise to a hydrophilic cavity capable of metal binding.[21] To reinforce the affinity of *per*-3,6-anhydro CDs for hard metal cations, their residual hydroxyl groups have been substituted by carboxymethyl groups. Recent development in our laboratory have involved the synthesis of the ligand hexakis(2-*O*-carboxymethyl-3,6,anhydro)-α-cyclodextrin named ACX (scheme 1) and the complexation study of $Lu^{3+}$ cation.[22] We have shown that this ligand was able to form mono- and binuclear complexes with $Lu^{3+}$ ions, and the crystal structure obtained for the $Lu_2(ACX)(H_2O)_2$ complex demonstrates the important role of the cavity in the lanthanide ion coordination.[22] Furthermore, the GdACX complex found an interesting application in magnetic resonance neuroimaging of tumor models on rats.

***Scheme 1.*** The Ligand ACX

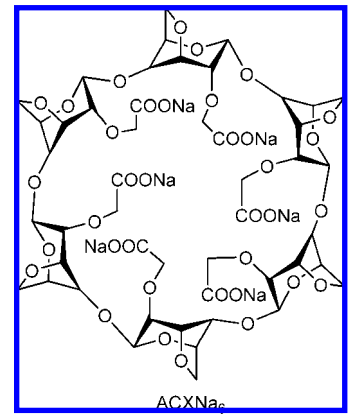


Indeed, this complex served to quantify an important tumor vasculature parameter, the cerebral blood volume, because it remains intravascular in the presence of the blood brain barrier lesions due to the tumor, in contrast to GdDOTA.[23] The fundamental interest of the coordination chemistry of $Ln^{3+}$ ions by biological molecule derivatives and the unexpected GdACX neuroimaging properties prompted us to a detailed study of the solution behavior of the $Ln^{3+}$ complexes of ACX.

The paper is organized as follows. The main features of the Grenoble method for dealing with electronic spin relaxation and relaxivity are described in the Theory section. An experimental and theoretical framework suitable for a rigorous interpretation of relaxivity data is exemplified by the GdACX complex in the user-friendly Results section.

## 2. Theory

In a paramagnetic solution the relaxivities of nuclear spins $I$ stem from their interactions with the electronic magnetic moments of the dissolved paramagnetic species. They give information about the statistical distribution and dynamics of these species with respect to the solvent or solute molecules bearing the observed nuclei. They gauge the efficiency of relaxation contrast agents (CAs) in MRI.

**2.1. Relaxivity. 2.1.1. Definitions and Macroscopic Equations.** The longitudinal and transverse relaxation rates $R_1 \equiv 1/T_1$ and $R_2 \equiv 1/T_2$ of a nuclear spin $I$ on a molecule $\mathcal{M}_I$ can be measured in an external magnetic field $\mathbf{B}_0$ by standard sequences.[24] Assume that $\mathcal{M}_I$ is in a solution of complexes GdL of a ligand L with the ion $Gd^{3+}$ of electronic spin $S = 7/2$. The relaxation rate $R_\alpha$ is the sum of the paramagnetic (p) relaxation

$$R_\alpha = R_{\alpha p} + R_{\alpha 0} \quad (\alpha = 1, 2) \tag{1}$$

rate $R_{\alpha p}$ due to the time-fluctuating Hamiltonian of the $I-S$ coupling and of the diamagnetic relaxation rate $R_{\alpha 0} \equiv 1/T_{\alpha 0}$, which originates from all the other fluctuating interactions acting on $I$ and is the value measured in the diamagnetic solution in the absence of GdL. The rate $R_{\alpha p}$, called the paramagnetic relaxation enhancement (PRE), is proportional to the concentration [GdL] of the complex, if the relaxation effects due to the individual complexes add up. Then, the relaxivity $r_\alpha$ ($s^{-1}$ $mM^{-1}$), defined as the increase of the PRE $R_{\alpha p}$ per mM of added complex, is independent of the GdL concentration. The reason

(10) Kowalewski, J.; Kruk, D.; Parigi, G. *Adv. Inorg. Chem.* **2005**, *57*, 41–104.
(11) Kowalewski, J.; Mäler, L., *Nuclear Spin Relaxation in Liquids: Theory, Experiments, and Applications*; Taylor and Francis: London, 2006.
(12) Schaefle, N.; Sharp, R. *J. Magn. Reson.* **2005**, *176*, 160–170.
(13) Aman, K.; Westlund, P. O. *Phys. Chem. Chem. Phys.* **2007**, *9*, 691–700.
(14) Fries, P. H.; Belorizky, E. *J. Chem. Phys.* **2007**, *126*, 204503.
(15) Belorizky, E.; Fries, P. H.; Helm, L.; Kowalewski, J.; Kruk, D.; Sharp, R. R.; Westlund, P.-O. *J. Chem. Phys.* **2008**, 052315.
(16) Connors, K. A. *Chem. Rev.* **1997**, *97*, 1325–1357.
(17) Yashiro, M.; Miyama, S.; Takarada, T.; Komiyama, M. *J. Inclusion Phenom. Mol. Recog.* **1994**, *17*, 393–397.
(18) Fatin-Rouge, N.; Bünzli, J.-C. G. *Inorg. Chim. Acta* **1999**, *293*, 53–60.
(19) Ashton, P. R.; Ellwood, P.; Staton, A.; Stoddart, J. F. *Angew. Chem., Int. Ed. Engl.* **1991**, *30*, 80–81.
(20) Gadelle, A.; Defayes, J. *Angew. Chem., Int. Ed. Engl.* **1991**, *30*, 78–80.
(21) Ashton, P. R.; Gattuso, G.; Königer, R.; Stoddart, J. F.; Williams, D. J. *J. Org. Chem.* **1996**, *61*, 9553–9555.
(22) Bonnet, C.; Gadelle, A.; Pécaut, J.; Fries, P. H.; Delangle, P. *Chem. Commun.* **2005**, 625–627.
(23) Lahrech, H.; Perles-Barbacaru, A.-T.; Aous, S.; Le Bas, J.-F.; Debouzy, J.-C.; Gadelle, A.; Fries, P. H. *J. Cereb. Blood Flow Metab.* **2008**, *28*, 1017–1029.
(24) Canet, D. *Adv. Inorg. Chem.* **2005**, *57*, 3–40.

why the effects of the individual GdL complexes on the PRE do not add up independently is manifold. For instance, increasing their concentration modifies the percentage of complexes engaged in some chemical association[3,5,25] and/or the physical properties of the solution. Such physical modifications can be a viscosity increase that slows down the molecular motions or an increase of the ionic strength that changes the Coulomb force between a charged GdL complex and a charged molecule $\mathscr{M}_I$, even at low GdL concentration.[26,27] Then, $R_{\alpha p}$ is no longer proportional to this concentration. However, for a given GdL concentration, an apparent relaxivity $r_\alpha$ can always be defined by eq 2 as the ratio of $R_{\alpha p}$ to [GdL].

$$r_\alpha \equiv R_{\alpha p}/[\mathrm{GdL}] = (R_\alpha - R_{\alpha 0})/[\mathrm{GdL}] \quad (2)$$

The fluctuating Hamiltonians that act on the nuclear spins and cause their relaxation have weak values and fast fluctuations, so that the Redfield theory is applicable to the description of the *nuclear* relaxation. A frequent situation is when the molecule $\mathscr{M}_I$ has a chemical exchange between the environment where it is bound to the complex and the environment where it diffuses freely. Assuming that the longitudinal and transverse nuclear relaxation times can be defined in both environments, Swift and Connick,[28] and Luz and Meiboom[29] obtained analytical expressions of the longitudinal and transverse PREs, or equivalently of the relaxivities. More precisely, the relaxivity $r_\alpha$ is the sum[2–4] in eq 3 of the IS contribution $r_\alpha^{IS}$ due to the complex bound to $\mathscr{M}_I$ and of the outer-sphere (OS) contribution $r_\alpha^{OS}$ stemming from the complexes, which diffuse freely with respect to $\mathscr{M}_I$.

$$r_\alpha = r_\alpha^{IS} + r_\alpha^{OS} \quad (3)$$

In the important case of the water protons, the IS relaxivity is given by[2–4] eq 4,

$$r_\alpha^{IS} = Pq/(T_{\alpha M} + \tau_M) \quad (4)$$

where $P \equiv 10^{-3}M/55.5M = 1.8 \times 10^{-5}$ is the ratio of the numbers of complexes and water molecules in the 1 mM solution of GdL complexes, $q$ is the number of water molecules coordinated to $Gd^{3+}$, $\tau_M$ is the residence time of such a coordinated water molecule, and $T_{\alpha M}$ is the intramolecular relaxation time of its protons in the absence of chemical exchange, i.e., the limiting situation where the water molecule would be coordinated to $Gd^{3+}$ for an infinite duration. Here, it should be emphasized that $T_{\alpha M}$ is defined within the framework of the Redfield theory of nuclear relaxation, i.e., the relaxation of the bound water protons has an exponential decay of characteristic time $T_{\alpha M}$ only for durations $\Delta t$ much longer than the correlation time $\tau_c$ of the fluctuating Hamiltonian $H_1(t)$ responsible for the relaxation. Thus, making use of $T_{\alpha M}$ is meaningless for a residence time $\tau_M < \Delta t$. In other words, the inequalities $\tau_c \ll \Delta t \leq \tau_M$ should be verified in order for eq 4 to hold. These inequalities also mean that the chemical exchange of water is not a fluctuation mechanism of the intramolecular Hamiltonian $H_1(t)$ at the origin of the nuclear relaxation of characteristic time $T_{\alpha M}$, so that $\tau_M$ should not appear in the definition of the correlation time $\tau_c$ of this Hamiltonian (see eqs 17 and 18). Finally, note that $r_\alpha^{IS} = 0$ in the absence of $\mathscr{M}_I$/GdL binding.

**2.1.2. IS Relaxivity.** Assume that the intramolecular relaxation rate $1/T_{1M}$ results from the fluctuations of the dipole−dipole Hamiltonian $H_{dip}(t)$ between $I$ and $S$. Since the beginning of the chemistry of contrast agents, many efforts have been devoted to the synthesis of $Gd^{3+}$ complexes with maximal $r_1^{IS}$ in order to increase the contrast efficiency.[2–4,30,31] More precisely, chemists have been modifying the molecular parameters involved in the popular Solomon-Bloembergen-Morgan (SBM) expression of $r_1^{IS}$ in order to reach the maximum of this expression. The Grenoble method is one of the rigorous theoretical frameworks providing reliable expressions for $r_1^{IS}$.[10,12,14,32–36] It will be presented hereafter together with the fundamental problems raised by the SBM approximation despite its reasonably successful application to the CAs at the imaging field values.

**2.1.2.1. Questionable Assumptions of the SBM Formalism.** Since the beginning of the theory of contrast agents,[30] $1/T_{1M}$ has been approximated by the SBM expression[2,3,10,11,15,37] in terms of the $Gd^{3+}$−water proton distance $r_H$, the rotational correlation time $\tau_r$ of the complex, and the longitudinal and transverse electronic spin relaxation times $T_{1e}$ and $T_{2e}$. However, the SBM expression rests on two major simplifying assumptions about the fluctuations of the ZFS Hamiltonian at the origin of the electronic spin relaxation: (i) the electronic spin relaxation and the Brownian rotation of the complex are uncorrelated (decomposition approximation[15]) and (ii) the fluctuations of the ZFS Hamiltonian can be handled by means of time-dependent second-order perturbation theory (Redfield theory[11,38]). The physical content of these assumptions is best understood by remembering that the ZFS Hamiltonian originates from the crystal field, which depends on the positions of the donor atoms coordinating $Gd^{3+}$ and acts on its 4f electrons via second-order perturbation effects of their spin−orbit coupling.[39] These assumptions were commonly accepted because it was thought that the ZFS fluctuations result only from the vibrations of the ligand atoms binding $Gd^{3+}$ and from the wagging of the coordinating water molecules and that these motions due to the collisions of the surrounding molecules with the complex are fast and uncorrelated with the tumbling orientation of the complex. However, it was realized that the average value of the ZFS Hamiltonian in a molecular (M) frame bound to the complex, the so-called "static" (in the molecular frame) ZFS Hamiltonian, gives rise to an electronic spin relaxation mechanism, necessary to properly interpret the multiple frequency and temperature EPR spectra of several $Gd^{3+}$ complexes.[7–9] This called for accurate theories of the intramolecular relaxation rate

(25) Vigouroux, C.; Bardet, M.; Belorizky, E.; Fries, P. H.; Guillermo, A. *Chem. Phys. Lett.* **1998**, *286*, 93–100.
(26) Fries, P. H.; Patey, G. N. *J. Chem. Phys.* **1984**, *80*, 6253–6266.
(27) Sacco, A.; Belorizky, E.; Jeannin, M.; Gorecki, W.; Fries, P. H. *J. Physique II France* **1997**, *7*, 1299–1322.
(28) Swift, T. J.; Connick, R. E. *J. Chem. Phys.* **1962**, *37*, 307–320.
(29) Luz, Z.; Meiboom, S. *J. Chem. Phys.* **1964**, *40*, 2686–2692.
(30) Lauffer, R. B. *Chem. Rev.* **1987**, *87*, 901–927.
(31) Avedano, S.; Tei, L.; Lombardi, A.; Giovenzana, G. B.; Aime, S.; Longo, D.; Botta, M. *Chem. Commun.* **2007**, 4726–4728.
(32) Benetis, N.; Kowalewski, J.; Nordenskiold, L.; Wennerstrom, H.; Westlund, P. O. *Mol. Phys.* **1983**, *48*, 329–346.
(33) Larsson, T.; Westlund, P. O.; Kowalewski, J.; Koenig, S. H. *J. Chem. Phys.* **1994**, *101*, 1116–1128.
(34) Rast, S.; Fries, P. H.; Belorizky, E.; Borel, A.; Helm, L.; Merbach, A. E. *J. Chem. Phys.* **2001**, *115*, 7554–7563.
(35) Abernathy, S. M.; Sharp, R. R. *J. Chem. Phys.* **1997**, *106*, 9032–9043.
(36) Schaefle, N.; Sharp, R. *J. Chem. Phys.* **2004**, *121*, 5387–5394.
(37) Bertini, I.; Luchinat, C.; Parigi, G. *Adv. Inorg. Chem.* **2005**, *57*, 105–172.
(38) Abragam, A., *Les Principes du Magnétisme Nucléaire*; PUF: Paris, 1961.
(39) Abragam, A.; Bleaney, B., *Résonance Paramagnétique Electronique des Ions de Transition*. PUF: Paris, 1971.

$1/T_{1M}$ dealing with the electronic spin relaxation beyond the SBM approximation.

**2.1.2.2. Grenoble Method for the IS Relaxivity.** The various available theoretical methods[10–12,14,32–36] were compared recently.[15] Here, the so-called Grenoble (G) method is applied to a real system for the first time and its key equations are briefly discussed. Complementary theoretical details can be found elsewhere.[14,15,34]

The G method consists in considering a large number $N_{or\text{-}vib} \cong 2000-100\,000$ of random realizations $j$ of the $Gd^{3+}$ complex with its IS water molecules, i.e., replicas of this complex, which are associated with a set of representative random initial orientations (or) and vibrational (vib) configurations and then undergo simulated rotational and vibrational Brownian motions. Let $\gamma_I$ be the gyromagnetic ratio of the nuclear spin $I$ and $\omega_I \equiv 2\pi\nu_I \equiv -\gamma_I B_0$ its angular Larmor frequency. Let $g_S$ be the Landé factor of the electronic spin $S$, $\gamma_S \equiv -g_S\mu_B/\hbar$ its gyromagnetic ratio, where $\mu_B$ is the Bohr magneton, and $\omega_S \equiv 2\pi\nu_S \equiv -\gamma_S B_0$ its angular Larmor frequency. In the (L) frame $Oxyz$ with $\mathbf{B}_0 // Oz$, let $\omega_S S_z$ be the Zeeman Hamiltonian of the $Gd^{3+}$ electronic spin $S$. Denote the ZFS Hamiltonian of the realization $j$ by $H^{(L)}_{ZFS,j}(t)$. The total Hamiltonian $H^{(L)}_{e,j}(t)$ acting on $S$ is given by eq 5.

$$H^{(L)}_{e,j}(t) = \omega_S S_z + H^{(L)}_{ZFS,j}(t) \tag{5}$$

The IS-PRE is determined[15,24] by the fluctuations of the dipolar magnetic field $\mathbf{B}_S$ created by the magnetic moment $\gamma_S\hbar\mathbf{S}$ of the electronic spin $S$ at the position of the nuclear spin $I$. More precisely, the longitudinal nuclear relaxation $1/T_{1M}$ due to these fluctuations is governed by the $-1$ standard component[40] $B_{S,-1j}(t)$ of $\mathbf{B}_S$, which is defined in terms of the $x$ and $y$ Cartesian components of $\mathbf{B}_S$ as $B_{S,-1}(t) \equiv [B_{S,x}(t) - iB_{S,y}(t)]/\sqrt{2}$. The operator $B_{S,-1j}(t)$ depends on the orientation of the complex and on the value of the ZFS Hamiltonian at time $t$. Its quantum expression is given in Supporting Information Appendix A. The IS time correlation function (TCF) $k^{IS}_{-1}(t)$ of this operator giving rise to the intramolecular relaxation rate $1/T_{1M}$ is defined as

$$k^{IS}_{-1}(t) \equiv \frac{1}{N_{or-vib}} \sum_{j=1}^{N_{or-vib}} \frac{1}{2S+1} \mathrm{Tr}_S\{[B_{S,-1j}(t)]^\dagger B_{S,-1j}(0)\} \tag{6}$$

The summation is a statistical average over all the realizations of the $Gd^{3+}$ complex. For a given complex, the correlation loss between $B_{S,-1j}(0)$ and $B_{S,-1j}(t)$ due to the evolution of the quantum states of the electronic spin $S$ is given by the matrix trace $\mathrm{Tr}_S$ that performs a quantum average over these states. The rate $1/T_{1M}$ is proportional to the Fourier transform of $k^{IS}_{-1}(t)$ and given by

$$1/T_{1M} = 2\gamma_I^2 \mathrm{Re}\int_0^\infty k^{IS}_{-1}(t)\exp(-i\omega_I t)\,\mathrm{d}t \tag{7}$$

**2.1.2.3. Fluctuating ZFS Hamiltonian.** In any (M) frame of the GdL complex, the instantaneous ZFS Hamiltonian $H^{(M)}_{ZFS}(t)$, given in eq 8, can be written as the sum of its static (S) mean value $H^{(M)}_{ZFS,S} \equiv \overline{H^{(M)}_{ZFS}(t)}$ independent of $t$ and of the transient (T) residual spread $H^{(M)}_{ZFS,T}(t) \equiv H^{(M)}_{ZFS}(t) - H^{(M)}_{ZFS,S}$ due to the collisions of the complex with the surrounding molecules.

$$H^{(M)}_{ZFS}(t) = H^{(M)}_{ZFS,S} + H^{(M)}_{ZFS,T}(t) \tag{8}$$

Only the contributions of rank 2 to $H^{(M)}_{ZFS,S}$ and $H^{(M)}_{ZFS,T}(t)$, which are generally considered to be dominant,[8,9] are retained here. The static ZFS Hamiltonian is conveniently formulated in the molecular frame ($P_S$) of its principal axes $Ox_Sy_Sz_S$, fixed in the complex, where it is denoted by $H^{(P_S)}_{ZFS,S}$. In this frame, if $S_{x_S}$, $S_{y_S}$, $S_{z_S}$ are the Cartesian components of $S$, it is defined by eq 9 in terms of the axial and rhombic parameters $D_S$ and $E_S$.

$$H^{(P_S)}_{ZFS,S} = D_S\left[S^2_{z_S} - S(S+1)/3\right] + E_S\left(S^2_{x_S} - S^2_{y_S}\right) \tag{9}$$

The overall strength of $H^{(P_S)}_{ZFS,S}$ is given by the ZFS magnitude $\Delta_S = \sqrt{(2D_S^2/3 + 2E_S^2)}$. The Brownian rotational motion of the realization $j$ is described by the 3D rotation $R^{(P_S)}_{jt}$ transforming the (L) frame into the ($P_S$) frame at time $t$. Turn to the expression in the (L) frame of the transient ZFS Hamiltonian $H^{(L)}_{ZFS,T}(t)$ generated by $H^{(M)}_{ZFS,T}(t)$. The changes of coordination sphere giving rise to $H^{(L)}_{ZFS,T}(t)$ are simply modeled as follows. It is assumed[15] that $H^{(L)}_{ZFS,T}(t)$ stems from a time-independent term $H^{(P_T)}_{ZFS,T}$ of rank 2, defined in its own principal molecular frame ($P_T$) different from ($P_S$), and having a Brownian pseudorotational motion of correlation time $\tau_v$ that represents the characteristic times of the vibrations (v) of the complex. Let $Ox_Ty_Tz_T$ be the axes of ($P_T$). As discussed below, it is sufficient to further assume that $H^{(P_T)}_{ZFS,T}$ has the simple axial form of eq 10.

$$H^{(P_T)}_{ZFS,T} = D_T\left[S^2_{z_T} - S(S+1)/3\right] \tag{10}$$

where $S_{z_T}$ is the component of $S$ along the $z_T$ axis of ($P_T$). The strength of $H^{(P_T)}_{ZFS,T}$ is given by the ZFS parameter $\Delta_T = \sqrt{(2/3)}D_T$. The transient pseudorotational (ps) motion of the realization $j$ is described in the same way as its true Brownian rotational diffusion at the origin of the fluctuations of the "static" ZFS Hamiltonian. It is defined by the pseudorotation $R^{(P_T)}_{jt}$ that results from the Brownian rotational diffusion of correlation time $\tau_v$ and transforms (L) into ($P_T$) at time $t$. In contrast to the expression of the static ZFS in eq 9, which involves axial and rhombic contributions, the generating Hamiltonian $H^{(P_T)}_{ZFS,T}$ of the transient ZFS defined by eq 10 has no rhombic term $E_T$. This simplification is justified because the fast modulation of $H^{(L)}_{ZFS,T}(t)$ can be handled by the Redfield theory, which predicts[8] that the electronic spin relaxation depends only on the magnitude $\Delta_T = \sqrt{(2D_T^2/3 + 2E_T^2)}$ irrespective of the values of $D_T$ and $E_T$.

Starting from the definitions (eqs 9 and 10) of the static and transient contributions to the total ZFS Hamiltonian in principle molecular frames, the tensorial expression[40] of the total ZFS Hamiltonian $H^{(L)}_{ZFS,Sj}(t)$ of the realization $j$ in the (L) frame is recalled in Supporting Information eq A7. The effects of the electronic spin relaxation on the relaxivity due to $H^{(L)}_{ZFS,Sj}(t)$ can be simulated as sketched in Appendix A. At medium and high field, they are taken analytically into account through an effective correlation time $\tau_{c1}$ as shown by eqs 14–18. In addition, partial but particularly relevant information[14] on electronic spin relaxation is given by the normalized longitudinal and transverse electronic TCFs $G^{nor}_{||}(t)$ and $G^{nor}_{\perp}(t)$, which are defined in the (L) frame as

$$G^{nor}_{||}(t) \equiv \langle S_z(t)S_z\rangle / \langle S_z(0)S_z\rangle \tag{11}$$

$$\text{with}\quad \langle S_z(t)S_z\rangle \equiv \frac{1}{N_{or-vib}} \sum_{j=1}^{N_{or-vib}} \frac{1}{2S+1} \mathrm{Tr}_S\{S_{zj}(t)S_z\}$$

and

$$G^{nor}_{\perp}(t) \equiv \langle S_+(t)S_-\rangle / \langle S_+(0)S_-\rangle \tag{12}$$

(40) Messiah, A., *Mécanique Quantique*; Dunod: Paris, 1972; Vol. II.

$$\text{with} \quad \langle S_+(t)S_-\rangle \equiv \frac{1}{N_{\text{or-vib}}}\sum_{j=1}^{N_{\text{or-vib}}}\frac{1}{2S+1}\text{Tr}_S\{S_{+j}(t)S_-\}$$

and can be also simulated. The relaxivity change due to electronic spin relaxation is fully determined by these TCFs if the decomposition approximation holds, which is the basic assumption of the SBM approximation.

**2.1.2.4. Failure of the SBM Approximation.** As detailed in Supporting Information Appendix A, this failure is caused by the static ZFS Hamiltonian, which gives rise to a statistical correlation between the fluctuations of the spatial terms and electronic spin components entering the expression of the dipolar local field. This complicated correlation depends on the direction $\hat{u}(\overrightarrow{\text{GdH}}) \equiv \overrightarrow{\text{GdH}}/\|\overrightarrow{\text{GdH}}\|$ of the interspin $I-S$ vector $\overrightarrow{\text{GdH}}$ in the ($P_S$) frame. At low field, for a given distance $\|\overrightarrow{\text{GdH}}\|$, this correlation gives rise to a strong dependence of $1/T_{1M}[\hat{u}(\overrightarrow{\text{GdH}})]$ on $\hat{u}(\overrightarrow{\text{GdH}})$, which is beyond the scope of the SBM approximation[10,11,15] and demonstrates the inadequacy of this formalism. Moreover, the SBM theory rests also on the assumption that the TCFs $G_{\|}^{\text{nor}}(t)$ and $G_{\perp}^{\text{nor}}(t)$ have monoexponential time decays, characterized by the longitudinal and transverse relaxation times $T_{1e}$ and $T_{2e}$, respectively. This simplification does not occur at low field for most of the $Gd^{3+}$ complexes in aqueous solutions, for which the validity condition[10,11,13,14] $\Delta_S\tau_r \ll 1$ of the Redfield approximation of the electronic spin relaxation does not hold, so that the time decays of $G_{\|}^{\text{nor}}(t)$ and $G_{\perp}^{\text{nor}}(t)$ strongly deviate from monoexponentiality.[13,14]

**2.1.2.5. IS Relaxivity for a Real System.** A fully satisfactory interpretation of the low-field IS relaxivity would require precise structural information about $\overrightarrow{\text{GdH}}$ and ($P_S$). On the road to accurate simulation of $Gd^{3+}$-based MRI contrast agents, recent molecular dynamics (MD) simulations, including many-body polarization interactions, have provided satisfactory coordination numbers and distances between the metal and the coordinating donor atoms.[41] Moreover, recent simulation of a $Gd^{3+}$-based MRI contrast agent in a discrete water solvent by Car−Parrinello (CP) MD has demonstrated that the time-averaged simulated structure around the metal ion can be in excellent agreement with crystallographic data, provided that the 4f electrons of this heavy ion are not included in the frozen electron core, but treated explicitly.[42] However, CPMD is very computer demanding and restricted to simulations of reasonably small complexes over durations of the order of a few picoseconds, so that the prediction of the structural isomerism, which has been observed for $Gd^{3+}$ chelates[43] and is probably crucial for GdACX, is still a difficult challenge. Besides, the accurate computation of accurate ZFS parameters by quantum chemistry methods is not a routine problem.[44] A simple conservative approach to overcome the absence of precise structural information about $\overrightarrow{\text{GdH}}$ and ($P_S$) is proposed now in order to interpret the low-field IS relaxivity. For a given distance $\|\overrightarrow{\text{GdH}}\|$, the relaxation rate $1/T_{1M}[\hat{u}(\overrightarrow{\text{GdH}})]$ varies between the extremum values taken when $\overrightarrow{\text{GdH}}$ is in the $z_S$ direction and when it is perpendicular to it, e.g., in the $x_S$ or $y_S$ directions.[45] Each water molecule coordinated to $Gd^{3+}$ has two protons, $H_1$ and $H_2$, with quite different directions of $\overrightarrow{\text{GdH}_1}$ and $\overrightarrow{\text{GdH}_2}$ in the ($P_S$) frame. For instance, if $\overrightarrow{\text{GdH}_1}$ is along $z_S$, $\overrightarrow{\text{GdH}_2}$ is nearly in the equatorial plane. Thus, if several water molecules are coordinated to $Gd^{3+}$, the situation where the directions $\hat{u}(\overrightarrow{\text{GdH}_p})$ of their various protons $H_p$ are almost uniformly distributed in all the directions of the molecular frame is highly probable. This statement is even more justified if the $Gd^{3+}$ complex exists as a mixture of several isomers with different coordination geometries. Therefore, the probability that the experimental relaxation rate $1/T_{1M}^{\text{exp}}$ deviates significantly from the mean value corresponding to a uniform distribution of the directions of $\overrightarrow{\text{GdH}}$ in the ($P_S$) frame should be small. Thus, it is proposed to approximate $1/T_{1M}^{\text{exp}}$ by the weighted average $1/\overline{T}_{1M}$, defined by eq 13, of the three theoretical values of $1/T_{1M}$ calculated for the directions $\hat{x}_S$, $\hat{y}_S$, $\hat{z}_S$ of the principal axes of ($P_S$) and having equal weights $w_{\hat{x}_S} = w_{\hat{y}_S} = w_{\hat{z}_S} = 1/3$.

$$\frac{1}{\overline{T}_{1M}} = w_{\hat{x}_S}\frac{1}{T_{1M}(\hat{x}_S)} + w_{\hat{y}_S}\frac{1}{T_{1M}(\hat{y}_S)} + w_{\hat{z}_S}\frac{1}{T_{1M}(\hat{z}_S)} \tag{13}$$

**2.1.2.6. Medium- and High-Field Limit of the IS Relaxivity.** The general expression of $1/T_{1M}$ given by eqs 6 and 7, which incorporate the fluctuations of $H_{e,j}^{(L)}(t) = H_{ZFS,Sj}^{(L)}(t) + H_{ZFS,Tj}^{(L)}(t)$, considerably simplifies at a sufficiently high field value[14,15] $B_0 \geq 0.2-0.3$ T. At sufficiently high field, it can be shown[8,14,15,45] that $G_{\|}^{\text{nor}}(t)$ has a very simple quasi-monoexponential decay $G_{\|}^{\text{nor}}(t) = \exp(-t/T_{1e}^{\text{McL}})$, where the McLachlan (McL) longitudinal electronic spin relaxation rate $1/T_{1e}^{\text{McL}}$ is the sum in eq 14 of the static and transient contributions $1/T_{1e,S}^{\text{McL}}$ and $1/T_{1e,T}^{\text{McL}}$ given by eqs 15 and 16.

$$\frac{1}{T_{1e}^{\text{McL}}} = \frac{1}{T_{1e,S}^{\text{McL}}} + \frac{1}{T_{1e,T}^{\text{McL}}} \tag{14}$$

$$\frac{1}{T_{1e,S}^{\text{McL}}} \equiv \frac{1}{25}[4S(S+1)-3]\Delta_S^2\tau_r\left[\frac{1}{1+\omega_S^2\tau_r^2} + \frac{4}{1+4\omega_S^2\tau_r^2}\right] \tag{15}$$

$$\frac{1}{T_{1e,T}^{\text{McL}}} \equiv \frac{1}{25}[4S(S+1)-3]\Delta_T^2\tau_v\left[\frac{1}{1+\omega_S^2\tau_v^2} + \frac{4}{1+4\omega_S^2\tau_v^2}\right] \tag{16}$$

Then, $1/T_{1M}$ becomes independent of the direction of $\overrightarrow{\text{GdH}}$ in the ($P_S$) frame and reduces to the medium- (med) and high-field expression

$$\frac{1}{T_{1M}^{\text{med-high-field}}} = A\frac{\tau_{c1}}{4\pi r_H^6}\frac{1}{1+\omega_I^2\tau_{c1}^2} \tag{17}$$

where $A \equiv (8\pi/5)\gamma_I^2 g_S^2\mu_B^2 S(S+1)$ is the dipolar coupling factor and $\tau_{c1}$ an effective correlation time defined as $1/\tau_{c1} \equiv 1/\tau_r + 1/T_{1e}^{\text{McL}}$. At sufficiently high field or for $Gd^{3+}$ complexes of low and medium molecular weights, the inequality $\tau_r \ll T_{1e}$ holds, so that $\tau_{c1} \cong \tau_r$.

The relaxivity characterization proposed in this work rests also on the interpretation of the transverse relaxivity $r_2$ measured

(41) Clavaguera, C.; Sansot, E.; Calvo, F.; Dognon, J. P. *J. Phys. Chem. B* **2006**, *110*, 12848–12851.
(42) Pollet, R.; Marx, D. *J. Chem. Phys.* **2007**, *126*, 181102.
(43) Woods, M.; Aime, S.; Botta, M.; Howard, J. A. K.; Moloney, J. M.; Navet, M.; Parker, D.; Port, M.; Rousseaux, O. *J. Am. Chem. Soc.* **2000**, *122*, 9781–9792.
(44) Reviakine, R.; Arbuznikov, A. V.; Tremblay, J. C.; Remenyi, C.; Malkina, O. L.; Malkin, V. G.; Kaupp, M. *J. Chem. Phys.* **2006**, *125*, 054110.
(45) Fries, P. H.; Belorizky, E. *J. Chem. Phys.* **2005**, *123*, 124510.

at high field and defined in eqs 2–4. At high field, $1/T_{2M}$ reduces to the simple medium- and high-field expression.

$$\frac{1}{T_{2M}^{\text{med-high-field}}} = A\frac{\tau_{c1}}{4\pi r_H^6}\left[\frac{2}{3}+\frac{1}{2}\frac{1}{1+\omega_I^2\tau_{c1}^2}\right] \quad (18)$$

The reason for investigating both the longitudinal and transverse relaxivities at high field is that the different dispersions of $1/T_{1M}$ and $1/T_{2M}$ with $\omega_I\tau_{c1}$ imply differences between $r_1^{IS}$ and $r_2^{IS}$, which provide information about the residence time $\tau_M$.[46] In contrast, as $B_0$ vanishes, $1/T_{2M}$ tends toward $1/T_{1M}$ because of the isotropy of our 3D space and does not convey additional information. In addition, low-field relaxation measurements with Stelar FFC relaxometers[47] have been restricted to $T_1$ until recently, even though $T_2^*$ studies can now be envisaged (Stelar private communication).

**2.1.3. OS Relaxivity. 2.1.3.1. Grenoble Method for the OS Relaxivity.** The OS relaxivity $r_1^{OS}$ of the protons of $\mathscr{M}_I$ (water or probe solute) can be reasonably approximated by a much simpler expression than that of the IS relaxivity as discussed now. The OS relaxivity can be calculated by considering a large number $N_{pair}$ of random realizations $j$ of the pair $\mathscr{M}_I$/GdL, i.e., replicas of this pair. These realizations have random initial configurations chosen to reproduce the $\mathscr{M}_I$/GdL pair distribution function[48] $g_{IS}$ in the solution and then undergo translational, rotational, and vibrational Brownian motions according to the detailed balance principle.[49–52] Let $N_{GdL}$ be the number of $Gd^{3+}$ complexes in the actual solution. The OS-TCF $k_{-1}^{OS}(t)$ giving rise to the OS relaxivity is proportional to the TCF of the component $B_{S,-1j}(t)$ of the local dipolar field due to $Gd^{3+}$ in the various pairs. It is given by eq 19

$$k_{-1}^{OS}(t) = N_{GdL}\frac{1}{N_{pair}}\sum_{j=1}^{N_{pair}}\frac{1}{2S+1}\text{Tr}_S\{[B_{S,-1j}(t)]^\dagger B_{S,-1j}(0)\} \quad (19)$$

where $B_{S,-1j}(t)$ depends on the $I-S$ interspin vector $\mathbf{r}_{jt}$ generated by the OS dynamics. The OS relaxivity considerably simplifies if the motion of $\mathbf{r}_{jt}$ and the rotation of the complex are uncorrelated. This happens for the popular Ayant, Belorizky, Hwang, and Freed (ABHF) model, [49,50] where the spins $I$ and $S$ are taken to be at the centers of the molecules $\mathscr{M}_I$ and GdL, approximated as hard spheres diffusing in a viscous continuum. In the (L) frame, let $(r_{jt},\theta_{jt},\phi_{jt})$ be the spherical coordinates of the interspin $I-S$ vector $\mathbf{r}_{jt}$ in the complex $j$. Introduce the orientation $\hat{r}_{jt}\equiv(\theta_{jt},\phi_{jt})$ of $\mathbf{r}_{jt}$ and the spherical harmonics $Y_{2q}(\hat{r}_{jt})$ that depend on this orientation. Define the dipolar TCFs $g_{2,q'q}(t)$ of the random functions $Y_{2,q}(\hat{r}_j)/r_j^3$ as the ensemble averages

$$g_{2,q'q}(t) = g_2(t)\delta_{q'q} = \left\langle [Y_{2,q'}(\hat{r}_{jt})^*/r_{jt}^3][Y_{2,q}(\hat{r}_{j0})/r_{j0}^3]\right\rangle \quad (20)$$

In Supporting Information Appendix B, it is shown that the OS relaxivity can be approximated by eq 21.

$$r_1^{OS} = A\text{Re}\int_0^\infty g_2(t)\left[G_{||}^{nor}(t)\exp(-i\omega_I t)+\frac{7}{3}G_\perp^{nor}(t)\right]dt \quad (21)$$

Since the precise calculation of the intermolecular dipolar TCF $g_2(t)$ is a very complicated task, it is often replaced by the Hwang and Freed (HF) function[50] $g_2^{HF}(t)$ corresponding to the simplified ABHF model. Such a simplification is all the more acceptable because the OS relaxation contribution is smaller than the IS contribution, as is the case for the GdACX complex with its four coordinated water molecules. Within the ABHF model, denote the minimum interspin distance by $a_{GdH}$. Let $D$ be the relative translational diffusion coefficient of the interacting molecules and $\tau \equiv a_{GdH}^2/D$ their translational correlation time. The HF-TCF $g_2^{HF}(t)$ is given by eq 22.

$$g_2^{HF}(t) = 10^{-6}N_A\frac{18}{\pi a_{GdH}^3}\int_0^\infty \exp\left(-\frac{t}{\tau}x^2\right)\frac{x^2\,dx}{81+9x^2-2x^4+x^6} \quad (22)$$

**2.1.3.2. Medium- and High-Field Limit of the OS Relaxivity.** The ABHF spectral density $j_{2c}^{OS}(\sigma)$ is given by eq 23.

$$j_{2c}^{OS}(\sigma) = \frac{10^{-6}N_A}{a_{GdH}D}\text{Re}\left[\frac{4+k}{3(9+9k+4k^2+k^3)}\right] \quad \text{with } k\equiv\sqrt{\sigma\tau} \quad (23)$$

At sufficiently high field, $G_{||}^{nor}(t)$ has the monoexponential decay $G_{||}^{nor}(t) = \exp(-t/T_{1e}^{McL})$ and the contribution to $r_1^{OS}$ involving $G_\perp^{nor}(t)$ becomes negligible because of the fast oscillations of this function.[14] Then, $r_1^{OS}$ simplifies to the ABHF expression eq 24.

$$r_1^{OS,\,\text{med-high-field}} = Aj_{2c}^{OS}(1/T_{1e}^{McL}+i\omega_I) \quad (24)$$

Similarly, the medium and high-field ABHF transverse relaxivity $r_2^{OS}$ is given by eq 25.

$$r_2^{OS,\,\text{med-high-field}} = A\left[\frac{2}{3}j_{2c}^{OS}(1/T_{1e}^{McL})+\frac{1}{2}j_{2c}^{OS}(1/T_{1e}^{McL}+i\omega_I)\right] \quad (25)$$

To interpret the relaxivity data, $r_1 = r_1^{IS}+r_1^{OS}$ is obtained at low field by using (i) eq 4 to compute $r_1^{IS}$ with $T_{1M}$ replaced by $\bar{T}_{1M}$ of eq 13, and (ii) eq 21 to compute $r_1^{OS}$. At medium and high field, eqs 4, 17, 18, 24, and 25 serve to calculate $r_1$ and $r_2$. In this field domain, the electronic spin relaxation is mainly due to the fluctuations of the transient ZFS Hamiltonian, so that eqs 17 and 18 are very similar to the popular SBM equations providing the IS relaxivities. Similarly, eqs 24 and 25 giving the OS relaxivities give nearly the same predictions as the standard OS expressions. This justifies the SBM approximation and the usual interpretation of relaxivity at medium and high field despite the presence of a static ZFS Hamiltonian. Note that the theoretical expressions of the longitudinal relaxivity in the rotating frame[24] $r_{1\rho}$ are derived from those of the transverse relaxivity $r_2$ by replacing the index 2 by $1\rho$.

**2.2. EPR.** EPR spectra in liquids depend on the transverse relaxation of the electronic spin due to the fluctuating ZFS Hamiltonian. The information, which they provide about this Hamiltonian, supports and completes that deduced from the low and medium-field relaxivity data. In an EPR experiment, the

(46) Nonat, A.; Fries, P. H.; Pecaut, J.; Mazzanti, M. *Chem. Eur. J.* **2007**, *13*, 8489–8506.
(47) Ferrante, G.; Sykora, S., Technical aspects of fast field cycling. In *Advances in Inorganic Chemistry - Including Bioinorganic Studies*, Eldik, R. v., Ed.; Elsevier: Amsterdam, 2005; Vol. 57, pp 405−470.
(48) Hansen, J.-P.; McDonald, I. R., *Theory of Simple Liquids*; Academic Press: New York, 1996.
(49) Ayant, Y.; Belorizky, E.; Alizon, J.; Gallice, J. *J. Phys. (Paris)* **1975**, *36*, 991–1004.
(50) Hwang, L. P.; Freed, J. H. *J. Chem. Phys.* **1975**, *63*, 4017–4025.
(51) Fries, P.; Belorizky, E. *J. Phys. (Paris)* **1978**, *39*, 1263–1282.
(52) Fries, P. H.; Belorizky, E.; Bourdin, N.; Cinget, F.; Gagnaire, D.; Gorecki, W.; Jeannin, M.; Vottero, P. *THEOCHEM-J. Mol. Struc.* **1995**, *330*, 335–345.

***Table 1.*** Global Stability Constants for Metallic Complexes of ACX at 298 K in Aqueous KCl 0.1 M[a]

| log $\beta_{mlh}$ | *m* | *l* | *h* | M = La | M = Gd | M = Lu | M = Ca | M = Zn | M = Cu |
|---|---|---|---|---|---|---|---|---|---|
| M(ACX) | 1 | 1 | 0 | 7.6(1) | 7.52(5) | 7.4(1) | 3.7(1) | 5.0(1) | 6.35(5) |
| M(ACX)H | 1 | 1 | 1 | 11.9(1) | 12.0(1) | 12.0(1) | 9.3(1) | 10.0(1) | 11.08(6) |
| $M(ACX)H_2$ | 1 | 1 | 2 | 15.7(1) | 15.8(1) | 15.7(1) | 13.7(1) | 14.5(1) | 15.25(7) |
| $M(ACX)H_3$ | 1 | 1 | 3 | 19.3(1) | 19.3(1) | 19.3(2) | 17.5(2) | 18.5(1) | 18.8(1) |
| M(ACX)(OH) | 1 | 1 | −1 | 0.4(2) | 0.4(2) | 1.3(1) | | | −0.6(1) |
| $M_2(ACX)$ | 2 | 1 | 0 | 11.7(1) | 11.5(1) | 10.8(3) | | 8.8(1) | 10.04(3) |
| $M_2(ACX)(OH)$ | 2 | 1 | −1 | | | 6.4(1) | | 1.8(1) | 4.6(1) |
| $M_2(ACX)(OH)_2$ | 2 | 1 | −2 | −2.2(1) | −0.2(1) | 1.5(1) | | | −1.7(1) |

[a] $\beta_{mlh} = [M_m(ACX)_lH_h]/[M]^m[ACX]^l[H]^h$.

paramagnetic solution placed in the external field $\mathbf{B}_0//Oz$ is also submitted to a weak orthogonal field $\mathbf{B}_1//Ox$ oscillating at the frequency $\omega$. The energy of $\mathbf{B}_1$ absorbed by the GdL complexes is proportional to the imaginary part of their susceptibility[38] $\chi''(\omega,\omega_S)$. Here, define the resonance or central (c) field $B_c \equiv \omega/|\gamma_S|$ as the field value corresponding to the angular frequency $\omega$ of $\mathbf{B}_1$. Let $G_\perp^{nor}(t,B_c)$ be the normalized transverse electronic TCF defined in eq 12 and calculated for this field value. In Supporting Information Appendix B, it is shown that the "absorption" function $\chi''(\omega,\omega_S)$ can be approximated by eq 26

$$\chi''(\omega,\omega_S) = \xi_a \mathrm{Re}\int_0^\infty G_\perp^{nor}(t,B_c)\exp(-i\omega t)\exp[i(\omega_S-\omega)t]\,dt \quad (26)$$

where $\xi_a$ is an intensity factor which can be freely adjusted in order to fit the experimental spectrum. The theoretical EPR spectrum is the derivative $d\chi''(\omega,|\gamma_S|B_0)/dB_0$. It depends on the structural ZFS parameters $D_S$, $E_S$, $D_T$ (or $\Delta_T$) and on the rotational and vibrational correlation times $\tau_R$ and $\tau_v$ through the TCF $G_\perp^{nor}(t,B_c)$ defined by eq 12. Let $s^{exp}(B_0)$ be the recorded spectrum. The structural ZFS parameters, the correlation times, the intensity factor $\xi_a$, and the parameters $\xi_0$, $\xi_1$ of a baseline correction $\xi_0 + \xi_1 B_0$ can be adjusted so that $d\chi''(\omega,|\gamma_S|B_0)/dB_0$ fits the corrected experimental spectrum $s^{exp}(B_0) + \xi_0 + \xi_1 B_0$. Mathematical details are provided in Supporting Information Appendix C to compute $\chi''(\omega,\omega_S)$ within the Redfield limit[8,9] and by the MC simulation method.

To sum up, the relaxivities $r_1$ and $r_2$ (or $r_{1\rho}$) depend on 10 parameters: (1) the number $q$ of coordinated water molecules, (2) the rotational correlation time $\tau_r$ of the $Gd^{3+}$ complex, (3) the Gd−H effective mean distance $r_H$ of the coordinated water molecules, (4) the coordination lifetime $\tau_M$, (5) the collision diameter $a_{GdH}$ of an OS water proton and $Gd^{3+}$, (6) the relative diffusion coefficient $D$ of the water molecule and the complex, (7−8) the structural parameters $D_S$, $E_S$ of the static ZFS, (9−10) the structural parameter $\Delta_T$ and vibrational correlation time $\tau_v$ of the transient ZFS. Of course, a prerequisite for a reliable relaxivity analysis of metal complexes with a new scaffold is their thorough analytical study in order to know their compositions, speciation diagrams, and structures. This basic identity information is necessary, but still insufficient, because the relaxivities depend on too many molecular parameters with possible compensating effects. Therefore, the determination of the maximal number of these parameters by complementary techniques is an essential part of a reliable framework to interpret the relaxivity data of a new type of metal complex. Such a framework is presented now.

## 3. Case Study: The GdACX Complex

**3.1. Speciation and Stability Constants of the Metal Complexes.** The potentiometric study of the ligand shows that ACX is a weak hexabase with the following protonation constants in KCl 0.1 M at 298 K: $pK_{a1} = 3.1(2)$, $pK_{a2} = 3.5(1)$, $pK_{a3} = 4.18(8)$, $pK_{a4} = 4.40(6)$, $pK_{a5} = 5.02(7)$, $pK_{a6} = 5.40(7)$.[22] The same protonation constants were obtained with NaCl and $Bu_4NCl$ used as ionic buffers indicating no influence of the cation onto the protonation properties of ACX.

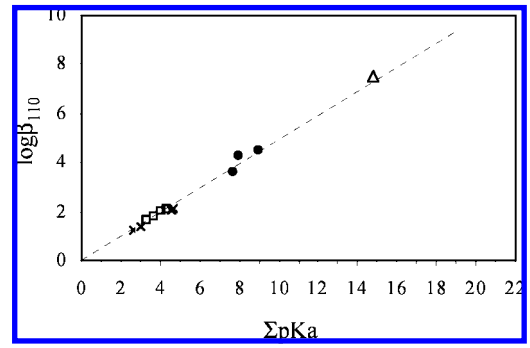


***Figure 1.*** Correlation between the affinity constants of the $Gd^{3+}$ complexes and the basicity ($\Sigma pK_a$) of a series of carboxylic ligands (×: acetate, chloroacetate, iodiacetate, propionate; ◆: benzoate, 3-nitrobenzoate, 3-fluorobenzoate, 4-methoxybenzoate; ●: phtalate, malonate, diethylmalonate). △ corresponds to ACX considered as a tridentate ligand ($\Sigma pK_a = 14.82$).

The complexes of three representative lanthanide cations, namely $La^{3+}$, $Gd^{3+}$, and $Lu^{3+}$, have been investigated in solution by potentiometry (298 K, 0.1 M KCl). The titration curves of $GdCl_3$/ACX solutions for different metal to ligand ratios are presented in Figure S1. Titration data for equimolar solution of $Gd^{3+}$ and the ligand could be satisfactorily fitted with the formation of several mononuclear complexes having different protonation states. In excess metal ion, the binuclear complex had to be considered. After the first end point, a second plateau is observed which is characteristic of the formation of soluble hydroxo complexes. The stability constants obtained for the different $Gd^{3+}$ complexes are given in Table 1.

The stability constant of the mononuclear $Gd^{3+}$ complex GdACX is $\log \beta = 7.5$ and is close to those obtained with tripodal ligands bearing three carboxylates as coordinating groups ($\log \beta_{R\text{-}TOTA\text{-}Gd} = 7.0(2)$).[53] Furthermore, it has been shown that for a series of similar ligands, the affinity for lanthanide ions is correlated to the basicity of the molecule, as the interaction is ionic.[54] Figure 1 shows the correlation between the affinity constants of a series of carboxylic ligands for the $Gd^{3+}$ cation and their basicity ($\Sigma pK_a$). If the molecule ACX is considered as a tridentate ligand ($\Sigma pK_a = 14.82$), the experimental affinity constant of the $Gd^{3+}$ complex is perfectly correlated with the regression line found for the mono- or diacides. This suggests that only three carboxylate functions

(53) Viguier, R.; Serratrice, G.; Dupraz, A.; Dupuy, C. *Eur. J. Inorg. Chem.* **2001**, 1789–1795.
(54) Choppin, G. R. *J. Alloys Compd.* **1997**, *249*, 1–8.

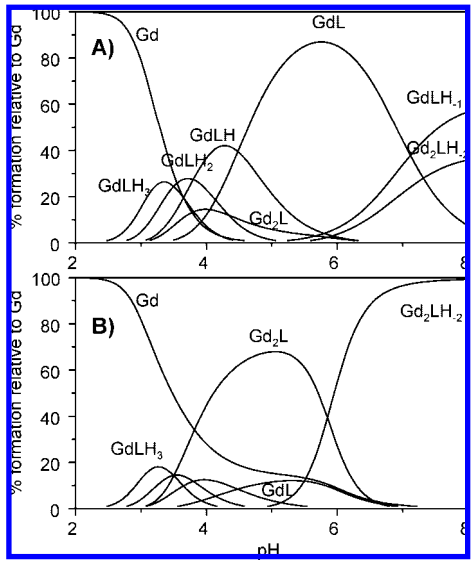


***Figure 2.*** Speciation diagramms of 1 mM ACX solution containing (A) 1 or (B) 2 equiv of $GdCl_3$. The stability constants tabulated in Table 1 were used to generate these diagrams.

are coordinated to the $Gd^{3+}$ ion in the mononuclear complex, leading to a structure similar to the one obtained in the solid state for the binuclear complex[22] but with only one compartment occupied by a lanthanide ion. Moreover, the mononuclear complex has three protonation constants ($pK_{a1} = 3.5$, $pK_{a2} = 3.8$, and $pK_{a3} = 4.48$), presumably corresponding to the protonation of the noncoordinating carboxylate functions. The stepwise formation constant of the binuclear complex ($K_2 = [Gd_2ACX]/[GdACX][Gd]$) is $\log K_2 = 3.9$ inferior to $\log \beta_{110} = 7.5$, showing that the introduction of a second cation is disfavored probably because of electrostatic repulsion between the two metal ions. The deprotonation of the $Gd^{3+}$ complexes occurs at relatively low pH. Indeed the hydrolysis constant of the GdACX complex, $\beta_{hyd} = [GdACX(OH)][H]/[GdACX] = 10^{-7.1}$ is lower than the hydrolysis constant of the aqua ion, $\beta_{hyd} = [Gd(OH)][H]/[Gd] = 10^{-8.39}$. Figure 2 displays the speciation diagrams of $Gd^{3+}$ complexes of ACX. In equimolar solutions of ACX and $Gd^{3+}$, the mononuclear complex GdACX is the major species in the pH range 5.5−6.5.

Similar results were obtained with $La^{3+}$ and $Lu^{3+}$, except in basic conditions where the $Lu^{3+}$ complexes were found to be more acidic (Figures S2−S3). No real trend is detected across the lanthanide series. Indeed, the $\log \beta_{110}$ are in the range 7.6−7.4 from La to Lu.

As expected, the introduction of carboxylate functions on the *per*-3,6-anhydrocyclodextrin scaffold allowed us to obtain lanthanide−CD complexes with enhanced stabilities. Indeed, the stability constant of the $Gd^{3+}$ complex of the natural α-CD is $\log \beta = 2.5(1)$.[18] *per*-3,6-Anhydro α-CDs bearing methyl instead of methylcarboxylate groups are also poor ligands of lanthanides.[55] The complexes LnACX are about 5 orders of magnitude more stable than the other CD complexes described in the literature.

It can be concluded here that the affinity constants found for the $Gd^{3+}$ complex of ACX, although greatly enhanced in comparison to natural CDs, is relatively modest. Indeed, if we calculate the pGd in usual conditions ($[Gd] = 10^{-6}$ M; $[ACX] = 10^{-5}$ M and pH 7.4) we find pGd = 8.9. Of course, this value is very low for using this complex in medical applications. However, it is interesting to note that this compound was injected to rodents despite its potential toxicity and that MRI images could be registered.[23] It has been demonstrated that release of $Gd^{3+}$ from the complex is responsible for the toxicity associated with $Gd^{3+}$ complexes. This release can be a consequence of $Zn^{2+}$, $Cu^{2+}$, and $Ca^{2+}$ transmetalation in vivo.[56] Therefore, the stability of the $Gd^{3+}$ complex is not sufficient to evaluate its toxicity but the selectivity for bioavailable cations has also to be taken into account. To determine the selectivity of this ligand for 4f over biologically relevant cations, we have investigated the thermodynamics of complexation of $Zn^{2+}$, $Cu^{2+}$, and $Ca^{2+}$ ions in solution by potentiometry (298 K, 0.1 M KCl) (Figures S4−S5), and calculated the affinity constants reported in Table 1. The comparison with classical polycarboxylate ligands shows that the selectivity for $Gd^{3+}$ over $Ca^{2+}$ is common, whereas the selectivity over $Zn^{2+}$ and especially $Cu^{2+}$ is larger.[57] Indeed, carboxylic ligands like malonate or polyaminocarboxylates like EDTA give higher affinity constants for $Cu^{2+}$ over $Gd^{3+}$. The selectivity of ACX for $Gd^{3+}$ over $Cu^{2+}$ and $Zn^{2+}$ may be attributed to the effect of the CD scaffold which places the carboxylate donor groups around a large cavity so that the coordination of large cations like $Ln^{3+}$ is more favorable than that of smaller ones like $Cu^{2+}$ and $Zn^{2+}$.

To take into consideration the competition of these bioavailable cations, Cacheris et al. have defined a $Gd^{3+}$ selectivity constant, called $K_{sel}$. This constant accounts for $Gd^{3+}$ selectivity of the ligand by modifying the thermodynamic stability constant of the $Gd^{3+}$ complex to incorporate ligand equilibrium with $H^+$, $Ca^{2+}$, $Zn^{2+}$, and $Cu^{2+}$.[56] Even though the stability of the GdACX complex is relatively low, its selectivity ($\log K_{sel}^{ACX} = 6.2$) is higher than that found for EDTA (for comparison $\log K_{sel}^{EDTA} = 4.2$, $\log K_{sel}^{DTPA} = 7.0$). Despite the fact that the toxicity of GdACX complex is far too high to consider it as a contrast agent for MRI, its selectivity for $Gd^{3+}$ over bioavailable divalent cations may explain why it could be injected to rodents to register MRI images.[23]

**3.2. Spectroscopic Structural Characterization. 3.2.1. NMR.** In order to get a better insight into the structure of the mononuclear and binuclear complexes, titrations of the ligand with various metallic salts were followed by $^1H$ NMR spectroscopy in $D_2O$. With $Ca^{2+}$, $Zn^{2+}$, and $La^{3+}$, the proton NMR signals of the ligand were slightly shifted and broadened, which is characteristic of rapid dynamic exchanges on the NMR time scale.

**3.2.1.1. Diamagnetic $Lu^{3+}$ Cation.** The titration of ACX with $Lu^{3+}$ (Figure S6) showed different features. The proton NMR signals are highly broadened when $Lu^{3+}$ is added to the CD ligand until a ligand-to-metal ratio of 1.5. This is typical of a dynamic process like for $Ca^{2+}$, $Zn^{2+}$, and $La^{3+}$. This process may be attributed to the intramolecular movement of the cation inside the ligand cavity; as all the carboxylate groups are not involved in the coordination of the cation, the latter can move from one coordination site (three adjacent carboxylate groups) to another equivalent coordination site. When more $Lu^{3+}$ is added, the spectrum changes dramatically and lots of resonances

(55) Baudin, C.; Tardy, F.; Dalbiez, J.-P.; Jankowski, C.; Fajolles, C.; Leclair, G.; Amekraz, B.; Perly, B.; Mauclair, L. *Carbohydr. Res.* **2005**, *340*, 131–138.

(56) Cacheris, W. P.; Quay, S. C.; Rocklage, S. M. *Mag. Reson. Imag.* **1990**, *8*, 467–481.

(57) Smith, R. M.; Martell, A. E.; Motekaitis, R. J. *NIST Critically Selected Stability Constants of Metal Complexes Database, NIST Standard Reference Database* **2001**, *46*.

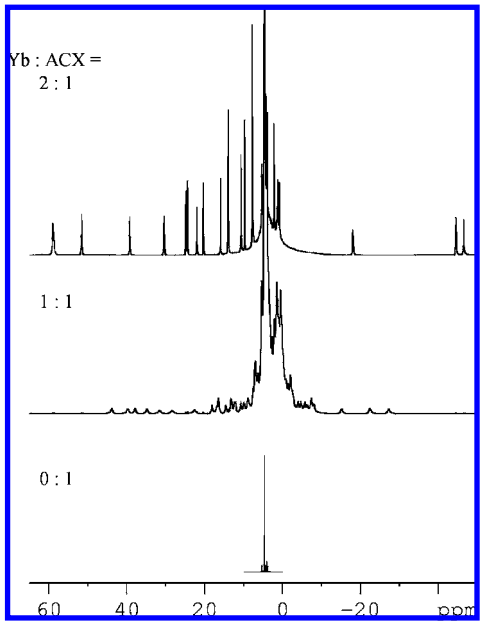


***Figure 3.*** 400 MHz proton NMR spectra during the titration of ACX with $Yb(OTf)_3$ in $D_2O$ at 298 K.

are detected. This spectrum (Figure S5) could be assigned with classical 2D NMR experiments (TOCSY, tROESY) to a $C_2$-symmetric complex in agreement with the solid state structure of $Lu_2ACX$ obtained by X-ray diffraction analysis.[22] The proton NMR resonances of this complex are sharp, and we can, therefore, conclude that the dinuclear complex structure is less dynamic than the structure of the mononuclear complex. Indeed, in $Lu_2ACX$, all the carboxylate functions of the ligand are coordinated to the metal ions and the intramolecular movements of the ions, if still possible, are greatly slowed. The $^{13}C$ spectrum of $Lu_2ACX$ also indicates a $C_2$ symmetry; in particular, three different resonances are detected for the carbon of the carboxylate functions.

**3.2.1.2. Paramagnetic $Ln^{3+}$ Ions.** The titration of ACX with $Yb^{3+}$ is presented in Figure 3 and shows similar features to the titration of $Lu^{3+}$, except that the $Yb^{3+}$ complexes are paramagnetic and therefore their proton NMR signals appear in a large range of chemical shifts. In default of $Yb^{3+}$, the spectrum is characteristic of a slow exchange on the NMR time scale (~0.1 ms) between the mononuclear complex and the free ligand. The complex YbACX displays more than 50 proton resonances in the chemical shift range −30 to 45 ppm, indicative of $C_1$ symmetry. This confirms that the cation is not at the center of the CD cavity and is not coordinated by all the carboxylate functions as it was deduced from the stability constants measured by potentiometry. When the metal to ligand ratio reaches more than 1 equiv, a second set of signals appears with higher paramagnetic chemical shifts, between −50 and 60 ppm. The $C_2$ symmetry of the dinuclear complex is confirmed by the number of resonances (27 = 54/2) detected in the proton NMR spectrum, indicating that the $Yb_2ACX$ complex has a similar structure to $Lu_2ACX$.

**3.2.2. EPR.** Interactions between paramagnetic metal ions such as $Gd^{3+}$ can be evidenced by EPR and more precisely by the variation of the electronic relaxation time related to the bandwidth of the EPR spectrum.[58] In order to have further proof of the existence of the binuclear complex and gain a better insight into the pH effect on the structure of these complexes, the EPR spectra of GdACX, $Gd_2ACX$, and $Gd_2ACX(OH)_2$ have been recorded at room temperature. Effective EPR line widths were obtained by fitting derivatives of Lorentzian functions to the experimental spectra: 250 (GdACX), 520 ($Gd_2ACX$), and 1000 G ($Gd_2ACX(OH)_2$). The broadening of the EPR lines in the binuclear complexes corresponds to relaxation due to Gd−Gd interaction (related to the distance between the two ions if dipolar) and to relaxation due to ZFS interactions. It has already been evidenced that the relaxation due to Gd−Gd interaction can be disregarded and only the relaxation due to ZFS interactions need to be considered if the paramagnetic $Gd^{3+}$ ion is replaced with a diamagnetic $Y^{3+}$ ion.[59] Given that the speciation and the stability constants are the same along the lanthanide series and since the ionic radii of $Gd^{3+}$ and $Y^{3+}$ are very similar (1.053 and 1.019 Å, respectively), the structure and the dynamic behavior of the two compounds in solution must be very similar. Since the diamagnetic $Y^{3+}$ complex has been doped with 10% of $Gd^{3+}$ ions, 95% of the $Gd^{3+}$ ions are found in the heterobimetallic complex, and the contribution of the homobinuclear $Gd^{3+}$ complex can be neglected. The 210 G broadening of the EPR peak line widths obtained for $Gd_2ACX$ (520 G) with regards to the GdYACX (310 G) can be clearly attributed to the formation of bimetallic complexes with close proximity of the paramagnetic centers. If we refer to the crystal structure obtained for the binuclear $Lu^{3+}$ complex, the corrected distance in the corresponding $Gd^{3+}$ complex should be 5.82 Å. This is consistent with the literature data where broadening of the EPR spectrum line widths have been observed at room temperature up to 6.79 Å.[59]

Unfortunately, it was not possible to measure an accurate EPR spectrum of $GdYACX(OH)_2$ because of the large line widths combined with the small concentration of $Gd^{3+}$ in the doped $Y^{3+}$ complexes. It is then impossible to conclude if the broadening observed in the bishydroxo complex $Gd_2ACX(OH)_2$ is only due to the presence of hydroxydes coordinated to the metal ion or could be attributed as well to the formation of a $\mu$-bridging bishydroxo complex causing the metal ions to come closer to each other. From a qualitative point of view, the 1000 G bandwidth observed in $Gd_2ACX(OH)_2$ remains very large compared to the 500−600 G bandwidths observed for complexes where the Gd−Gd distance is ca. 6.6 Å.[59]

**3.3. Qualitative High-Field Relaxivity.** At 4.7 T and above, the effects of the $Gd^{3+}$ electronic spin relaxation on the relaxivity only show up through the longitudinal electronic relaxation time $T_{1e}$ arising from the fluctuations of the transient ZFS Hamiltonian. This relaxation time, of the order [8,9] of 10 ns, is long enough to have negligible effect on the fluctuations of the nuclear-electron IS and OS dipolar coupling responsible for the relaxivity, so that the high-field eqs 17, 18, 24, and 25 of $r_\alpha^{IS}$ and $r_\alpha^{OS}$ hold with $T_{1e} \cong \infty$. Thus, the high-field water relaxivities depend only on the six parameters $q$, $\tau_r$, $r_H$, $\tau_M$, $a_{GdH}$, and $D$, which are clearly related to physicochemical properties that can be tailored by the chemist. More generally, the

(58) Powell, D. H.; Dhubhghaill, O. M. N.; Pubanz, D.; Helm, L.; Lebedev, Y. S.; Schlaepfer, W.; Merbach, A. E. *J. Am; Chem. Soc.* **1996**, *118*, 9333–9346.
(59) Nicolle, G. M.; Yerly, F.; Imbert, D.; Böttger, U.; Bünzli, J.-C.; Merbach, A. E. *Chem. Eur. J.* **2003**, *9*, 5453–5467.

***Table 2.*** Longitudinal Relaxivities $r_1$ of the Protons on Various Solute Probes at 298 K and 400 MHz due to the $GdACX^{3-}$ and $Gd(D_2O)_8^{3+}$ Complexes in $D_2O$ Solutions of 0.1 M KCl

| | $GdACX^{3-}$ | $Gd(H_2O)_8^{3+}$ |
|---|---|---|
| $r_1$ ($CH_3SO_3^-$) ($s^{-1}$ $mM^{-1}$) | 1.83(5) | 8.55(4) |
| $r_1$ (*t*-BuOD) ($s^{-1}$ $mM^{-1}$) | 1.57(5) | 1.72(1) |
| $r_1$ ($(CH_3)_4N^+$) ($s^{-1}$ $mM^{-1}$) | 1.95(1) | 0.77(1) |

simplified expressions of the high-field relaxivities in terms of molecular properties allow additional characterization of the complex.

**3.3.1. Water Proton Relaxivity.** It is essential to explore the concentration domain, where the water proton PRE $R_{1p}$ increases linearly with the concentration [GdL] of the complex in order to check the absence of chemical association. For GdACX, this was done in $H_2O$ with the supporting electrolyte KCl 0.1 M at pH 6. The values measured on a Varian Mercury-400 are reported in Table S1. In the concentration range 0.2−2 mM in $H_2O$ KCl 0.1 M, the longitudinal relaxivity is shown to have the constant value $r_1 \cong 22.4$ $s^{-1}$ $mM^{-1}$ at 400 MHz and 298 K. This high value was unexpected since only one water molecule is coordinated to the lanthanide cation in the solid state structure of the binuclear $Lu^{3+}$ complex.[22] Clearly, complementary investigations are needed to interpret these relaxivity data. Unless otherwise explicitly stated, the additional experimental studies were carried out in $H_2O$ with KCl 0.1 M at 298 K, pH 6.

**3.3.2. Intermolecular Probe Relaxivity.** $T_1$ measurements of nuclear spins $I$ on intermolecular probes can give access to dynamic and structural parameters of the complex. The use of noncoordinating probes has already proven its interest in the determination of transmetalation equilibrium constant.[60] Indeed, OS relaxation stems from the modulation of the dipolar coupling between the observed nuclear spin $I$ and the $Gd^{3+}$ electronic spin $S$. The magnitude of this coupling depends on the $I-S$ minimal distance of approach[2,3] and on the electrostatic interactions between the probe and the complex.[26,27] Its modulation is governed by the relative translational diffusion of the two species.[2,3] We chose three probes, methanesulfonate ($MS^-$), *tert*-butanol (*t*-BuOH), and tetramethylammonium ($TMA^+$), having similar sizes and relative translational dynamics with respect to GdACX, but bearing different charges in order to investigate the local electric charge of the $Gd^{3+}$ coordination site on the complex. Their proton relaxation rates $R_1$ were measured at 400 MHz for a fixed ACX concentration but increasing $Gd^{3+}$ concentrations (ligand titration with $Gd^{3+}$) in $D_2O$ solutions of 0.1 M KCl. Before 1 equiv of added $Gd^{3+}$, the PRE depends linearly on [$Gd^{3+}$], which agrees with the presence of only one species in solution, GdACX. The relaxivities obtained with the various probes in the presence of GdACX are reported in Table 2 together with those measured in the presence of $Gd(D_2O)_8^{3+}$ for comparison. In the case of $Gd(D_2O)_8^{3+}$, as expected from the change from Coulomb attraction to repulsion, the relaxivity decreases in the order negatively charged $MS^-$ > neutral *t*-BuOH > $TMA^+$. For the globally anionic $GdACX^{3-}$, even if the highest relaxivity is observed for the positively charged $TMA^+$ as expected, the relaxivities of the three probes are very similar. The much smaller Coulomb effects found for $GdACX^{3-}$ can be explained as follows. The $Gd^{3+}$ cation is less accessible to the intermolecular probes in the large GdACX complex than in the $Gd(D_2O)_8^{3+}$ complex, and the ACX carboxylate negative charges are more delocalized than the 3+ charge of the free $Gd^{3+}$ aqua ion. Moreover, the fact that the PREs of the probes are nearly independent of their charges is characteristic of a local neutral charge of the $Gd^{3+}$ coordination site of $GdACX^{3-}$. This confirms that $Gd^{3+}$ is coordinated by three carboxylate groups that exactly compensate the +3 charge of the cation, as already deduced from the value of the stability constant. In summation, the probes approach a neutral compartment containing $Gd^{3+}$ and slightly sense the negative charge of the complex due to the other three carboxylate functions that are far away from the paramagnetic ion.

**3.4. Number of Metal-Bound Water Molecules.** According to eq 4, the number $q$ of the water molecules bound to each complexed $Gd^{3+}$ governs the IS contribution to the relaxivity. For a new ligand like ACX, the geometry of which creates nontrivial spatial coordination constraints, reliable chemical intuition on the ligand denticity and hydration state is made very difficult. Thus, an independent experimental determination of $q$ is highly desirable. Measurements of $Eu^{3+}$ and $Tb^{3+}$ luminescence lifetimes in solution were performed in order to obtain the hydration state of the lanthanide ion in the mononuclear complex. Due to the different quenching efficiencies of the O−H and O−D oscillators, the measurements of $Eu^{3+}$ or $Tb^{3+}$ luminescence lifetimes $\tau_{lum}$ of the excited-state of the complex in $H_2O$ and $D_2O$ allows an estimation of $q$. The empirical equations of Parker and co-workers,[61] which are corrected versions of the equations of Horrocks and Sudnick[62,63] accounting for closely diffusing OH oscillators can then be used. The results obtained for the two complexes (1 mM LnACX, in KCl 0.1 M) are reported in Table S2. The calculated numbers of coordinated water molecules are between 4 and 5. As the Horrocks equations have been determined for complexes having from 0 to 9 IS water molecules, they are more suitable for high hydration states. Therefore, we can expect $q$ to be closer to 4 than 5 in LnACX complexes. This indicates that the environment of the metal ion in the mononuclear complex is totally different from that expected from the solid-state structure of the complex $Lu_2ACX(H_2O)_2$. Indeed, a hydration number of 4 implies that some coordination bonds with the CD scaffold, probably with the oxygen atoms of ether linkages, are disrupted in solution, leading to a $Gd^{3+}$ ion exposed to the solvent.

**3.5. Self-Diffusion Coefficient of the Complex.** The self-diffusion coefficient $D_S^t$ of a $Ln^{3+}$ complex gauges the speed of its translational (t) Brownian dynamics. It depends on its van der Waals radius $a_S$ and the solution viscosity $\eta$ via the Stokes−Einstein eq 27 corrected by a translational microviscosity factor $f_S^t$ that accounts for the discrete nature of the solution [6,8]

$$D_S^t = k_B T/(6\pi a_S \eta f_S^t) \quad (27)$$

The self-diffusion coefficient of a complex with the diamagnetic $Lu^{3+}$ can be measured by $^1H$ pulsed gradient spin echo (PGSE) NMR. It gives information on its hydrodynamic radius $a_S^{hyd} = a_S f_S^t$, which can corroborate the chemical composition, structure, and association properties obtained by other techniques. At 298 K, the measured value of the self-diffusion

(60) Bonnet, C. S.; Fries, P. H. *Magn. Reson. Chem.* **2003**, *41*, 782–787.
(61) Beeby, A.; Clarkson, I. M.; Dickins, R. S.; Faulkner, S.; Parker, D.; Royle, L.; de Sousa, A. S.; Williams, J. A. G.; Woods, M. *J. Chem. Soc., Perkin Trans.* **1999**, *2*, 493–503.
(62) Horrocks, W.; De, W., Jr.; Sudnick, D. R. *J. Am. Chem. Soc.* **1979**, *101*, 334–340.
(63) Horrocks, W.; De, W., Jr.; Sudnick, D. R. *Acc. Chem. Res.* **1981**, *14*, 384–392.

coefficient of LuACX in $D_2O$ is $D_S^t(D_2O) = 0.25 \times 10^{-5}$ cm$^2$ s$^{-1}$. According to the Stokes−Einstein formula, the value in $H_2O$, which scales with the viscosity ratio $\eta(D_2O)/(H_2O) = 1.24$, is calculated to be $D_S^t(H_2O) = 0.31 \times 10^{-5}$ cm$^2$ s$^{-1}$. The radius $a_S$ was evaluated from the X-rays solid state structure of the binuclear $Lu^{3+}$ complex,[22] by considering a sphere having the same volume as the ellipsoid that best approximates this structure. Let $d_1 = 13.5$ Å, $d_2 = 12.6$ Å, and $d_3 = 9.5$ Å be the lengths of the principal axes of the ellipsoid approximating the complex as defined by a CPK compact molecular model. The radius of the sphere having the same volume is simply $a_S = 0.5(d_1d_2d_3)^{1/3} = 5.9$ Å. The hydrodynamic radius $a_S^{hyd} = 7.9$ Å derived from eq 23 leads to a microviscosity factor $f_S^t = 1.35$ larger than 1 and consistent with the ACX hydrophilic character, which implies that ACX is accompanied in the course of its motion by a shell of loosely bound water molecules.

**3.6. Rotational Correlation Time from $^2$H Longitudinal Relaxation.** The rotational correlation time of a complex is defined as $\tau_r \equiv 1/(6D_S^r)$, where $D_S^r$ is its rotational diffusion coefficient that can be calculated via the rotational Stokes−Einstein eq 28

$$D_S^r = k_B T/(8\pi a_S^3 \eta f_S^r) \tag{28}$$

$f_S^r$ being the rotational microviscosity factor of the complex. Rough estimates of $\tau_r$ can be obtained at 298 K in $H_2O$ from the previous self-diffusion study through different applications of eq 28. First, using the corrected Gierer and Wirtz eq 43 of ref 8 to calculate $f_S^r = 0.53$, we obtain $\tau_r = 97$ ps. Second, assuming that the LnACX hydrodynamic radius is $a_S^{hyd} = 7.9$ Å, the rotational diffusion coefficient becomes $D_S^r = k_BT/(8\pi a_{S,hyd}^3\eta)$ and $\tau_r = 557$ ps. Third, under the tempting ad hoc hypothesis that the rotational and translational microviscosity factors are equal, i.e., $f_S^r = f_S^t = 1.35$, we have $\tau_r = 247$ ps. Clearly, reliable predictions about diffusion coefficients are more difficult with hydrophilic ligands like ACX than with polyaminocarboxylate ligands.[6,8] Direct experimental determination of $\tau_r$ for a metal complex with a new scaffold is a key step of a safe characterization. This can be carried out by longitudinal $^2$H relaxation rate measurements on a deuterated analogue of the diamagnetic $La^{3+}$ or $Lu^{3+}$ complex.[3] For ACX, the ligand is deuterated in position 7. In solution, the $^2$H longitudinal relaxation rate $1/T_1(^2H)$ is governed by the fluctuations of the electric field gradient that acts on the nucleus and fluctuates because of the Brownian rotation of the complex. Let $I' = 1$ be the deuterium nuclear spin and $\chi$ its quadrupolar coupling constant, taken to be 170 kHz.[6] The rate $1/T_1(^2H)$ reads

$$1/T_1(^2H) = \frac{3\pi^2}{10}\frac{2I'+3}{I'^2(2I'-1)}\chi^2\tau_r \tag{29}$$

if the small effects of the nuclear asymmetry parameter are neglected. The spectra of the deuterated ligand or its $La^{3+}$ mononuclear complex show one resonance with a line width of 30−40 Hz at 298 K. The rotational correlation time obtained though eq 29 from the measured relaxation time $T_1(^2H) = 9.0$ ms is $\tau_r = 260$ ps, in fair agreement with the value 247 ps derived from the self-diffusion study by applying the Stokes−Einstein equations under the hypothesis of equal rotational and translational microviscosity factors. Again, the high value of the rotational microviscosity factor $f_S^r = 1.42$ leading to $\tau_r = 260$ ps for a van der Waals radius $a_S = 5.9$ Å via eq 28 shows the strong hydrophilic nature of ACX.

**3.7. Quantitative High-Field Relaxivity.** When the IS contribution dominates the water relaxivity because the complex GdL tumbles slowly and/or has a large hydration state, the OS contribution has a minor effect and can be satisfactorily approximated by the ABHF model with a typical minimal OS distance of approach $a_{GdH} = 4$ Å between $Gd^{3+}$ and the water hydrogen nucleus. Such a situation occurs for GdACX. Then, the OS relaxivities $r_\alpha^{OS}$ can be calculated from eqs 24 and 25, where the relative diffusion coefficient $D$ is the sum of the self-diffusion coefficients of water and GdL previously determined by PGSE NMR techniques. When the OS contribution becomes significant, note that it can be derived experimentally with the help of noncoordinating probe solutes mimicking the OS behavior of water.[46] The high-field IS relaxivity depends on the four parameters $q$, $\tau_r$, $r_H$, and $\tau_M$. Since $q$ and $\tau_r$ can be obtained from independent luminescence lifetime and $^2$H relaxation studies, only $r_H$ and $\tau_M$ remain to be determined. This can be done from the experimental values of $r_1$ and $r_2$ (or $r_{1\rho}$) at a given field. The relaxivity values due to GdACX (0.95 mM) were measured at 400 MHz and 298 K on a Varian Unity spectrometer. They are $r_1 = 22.9$ s$^{-1}$ mM$^{-1}$ and $r_2 \cong r_{1\rho} = 35.5$ s$^{-1}$ mM$^{-1}$, so that the IS relaxivities are $r_1^{IS} = (r_1 - r_1^{OS}) = 21.6$ s$^{-1}$ mM$^{-1}$, $r_2^{IS} = (r_2 - r_2^{OS}) = 33.8$ s$^{-1}$ mM$^{-1}$. Using the typical mean value $r_H = 3.1$ Å for the IS Gd−H distance,[64] their theoretical counterparts calculated from eqs 4, 17, and 18 agree to within ≅5% for any short water residence time $\tau_M \leq 100$ ns. Since $T_{1M} = 3.1$ $\mu$s and $T_{2M} = 2.2$ $\mu$s, $\tau_M$ is too short to have a sizable effect on the relaxivity and needs not to be determined by more accurate $^{17}$O studies.[2,65] Also, note that the water PREs do not increase linearly with the GdACX concentrations above 10 mM required by such studies (see Section 3.9). So far, we have been able to determine all the parameters governing the high-field relaxivity. The ZFS parameters, which affect the low and medium field relaxivity, can be obtained from NMRD and EPR studies.

**3.8. NMRD Profile and EPR.** The effects of the fluctuating static and transient ZFS Hamiltonians on relaxivity through electronic spin relaxation decrease with field, roughly as $\tau_r/(1 + \omega_S^2\tau_r^2)$ and $\tau_v/(1 + \omega_S^2\tau_v^2)$, respectively. Since these Hamiltonians have similar magnitudes and $\tau_r \gg \tau_v$, the influence of the static ZFS, which dominates at low field, vanishes in the field domain $B_0 \geq 0.2-0.3$ T, where the transient ZFS becomes the main cause of electronic spin relaxation effects. The situation is similar with EPR spectroscopy. The transverse electronic TCF is more affected by the static ZFS Hamiltonian than by its transient counterpart at low field, whereas the reverse is true at higher field.[8] The $r_1$ profile measured with the help of a Stelar fast field cycling (FFC) relaxometer between 30 kHz and 35 MHz is displayed in Figure 4 where the value at 400 MHz is also reported. The EPR spectrum at X band (9.766 GHz) is shown in Figure 5. The yet unknown parameters $D_S$, $E_S$, $\Delta_T$, and $\tau_v$ were simultaneously adjusted so that the theoretical $r_1$ expression given by eqs 3, 4, 6, 7, 13, and 21 and the theoretical EPR spectrum $d\chi''(\omega,|\gamma_S|B_0)/dB_0$ with $\chi''(\omega,|\gamma_S|B_0)$ given by eq 26 fit their experimental counterparts as shown in Figures 4 and 5. The adjusted ZFS parameters are $D_S = 0.96\Delta_S$ and $E_S = 0.20\Delta_S$ with $\Delta_S = 0.45 \times 10^{-10}$ rad s$^{-1}$, $\Delta_T = 0.34 \times 10^{-10}$ rad s$^{-1}$, $\tau_v = 8$ ps, in reasonable agreement with previously published values.[8,9] The Landé factor of the $Gd^{3+}$ electronic spin was also slightly adjusted to the value $g_S = 1.985$. Finally, the reasonable estimate[64] $r_H = 3.14$ Å was found for the optimal IS Gd−H distance. The theoretical relaxivity represented by

(64) Caravan, P.; Astashkin, A. V.; Raitsimring, A. M. *Inorg. Chem.* **2003**, *42*, 3972–3974.
(65) Merbach, A. E.; Vanni, H. *Helv. Chim. Acta* **1977**, *60*, 1124–1127.

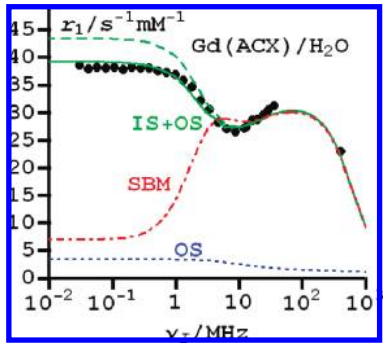


***Figure 4.*** Water proton longitudinal relaxivity $r_1$ ($s^{-1}mM^{-1}$) due to GdACX at 298 K in $H_2O$, KCl 0.1 M. The theoretical relaxivity was calculated for two different distributions of the $Gd^{3+}$−water hydrogen directions in the principal frame of the static ZFS Hamiltonian: isotropic distribution (dashed curve) and distribution with preferred orientation (continuous curve). The dash-dotted curve is the relaxivity profile derived from the SBM approximation.

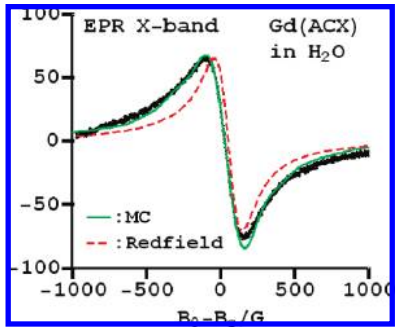


***Figure 5.*** X-band EPR spectrum of GdACX at 298 K in $H_2O$, KCl 0.1 M with $B_c = 3515.2$ G.

the dashed curve in Figure 4 was calculated under the conservative hypothesis that the directional relaxation rates $1/T_{1M}(\hat{u})$ in eq 13 have equal weights $w_{\hat{u}}$ for the three principal axes $\hat{u} = \hat{x}_S, \hat{y}_S, \hat{z}_S$ of the static ZFS Hamiltonian. However, in a real complex, the water molecules bound to $Gd^{3+}$ are expected to be located only in a restricted region of the coordination sphere, so that the $Gd^{3+}$−water hydrogen vectors $\overrightarrow{GdH}$ should have a preferred direction with respect to the principal frame ($P_S$). In Figure 4, the continuous curve is the theoretical relaxivity calculated with $w_{\hat{x}_S} = 0.5$, $w_{\hat{y}_S} = 0.3$, $w_{\hat{z}_S} = 0.2$ in eq 13 and accounting for a preferred direction of $\overrightarrow{GdH}$ along $\hat{x}_S$. The agreement with experiment is very satisfactory.

According to the usual IS and OS models, the high water relaxivity values induced by the GdACX complex can be simply attributed to the high hydration state of the complex associated with a medium-range rotational correlation time.

Finally, the predictions of the standard theory based on the Redfield approximation of the electronic spin relaxation are compared with the Grenoble results for the same molecular parameters. In Figure 5, the difference is significant for the Redfield EPR spectrum at X-band, which corresponds to a medium field value $B_0 \cong 0.35$ T. In Figure 4, it becomes dramatic at low field for the relaxivity profile derived from the SBM approximation because the electronic spin relaxation due to the fluctuating static ZFS Hamiltonian is much too fast and quenches the relaxivity in an unphysical way. On the other hand, at the imaging field values and above, the SBM approximation is satisfactory as discussed above.

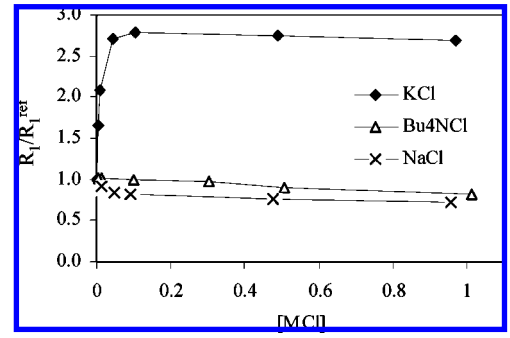


***Figure 6.*** Evolution of the water proton relaxation rate in a solution of GdACX in water at 400 MHz and 298 K, as a function of the concentration of the electrolyte MCl, M = K, Na, or $Bu_4N$. $R_1^{ref}$ is the water proton relaxation rate in pure water.

**3.9. Validity Range of the Speciation Model.** It should be noted that in addition to $r_1$ all the properties $q$, $D$, and $\tau_r$ investigated in KCl 0.1 M are constant in the GdACX concentration range 0.1−3 mM. Nevertheless, some striking changes have been detected when increasing the GdACX concentration or changing the supporting electrolyte.

**3.9.1. Concentration Effects.** For higher concentrations (10−30 mM) of GdACX, a decrease of the water relaxivity, correlated to a decrease of the number of IS water molecules from 4 to 2, was observed. Indeed, the number of coordinated water molecules measured by $^{17}O$ NMR of the $Dy^{3+}$ complex (30 mM) was $q_{Dy} = 2$ (Figure S9). This value was confirmed by luminescence lifetime measurements in a 10 mM $Tb^{3+}$ complex solution, which also gave $q_{Tb} = 2$. In concentrated (10−30 mM) complex solution, the translational self-diffusion coefficient of the complex also decreases and the rotational correlation time obtained from $^2H$ NMR experiments increases of about 20%. These data are consistent with the formation of aggregates when the complex concentration reaches 10 mM. Moreover, CD aggregation for concentrations above 10 mM has already been reported.[66–68] In contrast to the usual increase of water relaxivity due to aggregation with increased concentration of the complex, because of the lengthening of $\tau_r$,[69–71] the aggregation of GdACX complexes leads to a decrease of the number of coordinated water molecules in the hindered aggregates and, therefore, to a correlated decrease of the relaxivity.

**3.9.2. Effect of the Supporting Electrolyte.** Whereas the electrolyte salt has no significant effect on the stability constants of the $Gd^{3+}$ complexes as measured by potentiometry, longitudinal water proton relaxivity was found to be very sensitive to the presence or absence of $K^+$ (Figure 6).

It is clear that the $Na^+$ and $Bu_4N^+$ cations have no significant effect on the water relaxation rates, whereas $K^+$ induces a great

(66) Coleman, A. W.; Nicolis, I. *J. Inclusion Phenom. Mol. Recog.* **1992**, *13*, 139–143.
(67) Gonzalez-Gaitano, G.; Rodriguez, P.; Isasi, J. R.; Fuentes, M.; Tardajos, G.; Sanchez, M. *J. Inclusion Phenom. Mol. Recog.* **2002**, *44*, 101–105.
(68) Bonini, M.; Rossi, S.; Karlsson, G.; Almgren, M.; LoNostro, P.; Baglioni, P. *Langmuir* **2006**, *22*, 1478–1484.
(69) Laus, S.; Sitharaman, B.; Toth, E.; Bolskar, R. D.; Helm, L.; Asokan, S.; Wong, M. S.; Wilson, L. J.; Merbach, A. E. *J. Am. Chem. Soc.* **2005**, *127*, 9368–9369.
(70) Toth, E.; Bolskar, R. D.; Borel, A.; Gonzalez, G.; Helm, L.; Merbach, A. E.; Sitharaman, B.; Wilson, L. J. *J. Am. Chem. Soc.* **2005**, *127*, 799–805.
(71) Costa, J.; Balogh, E.; Turcry, V.; Tripier, R.; Baccon, M. L.; Chuburu, F.; Handel, H.; Helm, L.; Toth, E.; Merbach, A. E. *Chem. Eur. J.* **2006**, *12*, 6841–6851.

enhancement with a plateau reached for a concentration of 0.1 M. As self-diffusion and rotational correlation time $\tau_r$ do not change upon addition of $K^+$, this observation cannot be attributed to aggregation. On the other hand, this dramatic change in water relaxivity is correlated to an evolution of the number of water molecules coordinated to the $Ln^{3+}$ ion from $q = 0.5$ to 1 in the absence of $K^+$ to $q = 4$ in the presence of $K^+$. These data suggest that in the absence of $K^+$, the coordination environment of $Ln^{3+}$ is similar to that evidenced in the solid-state structure of $Lu_2ACX(H_2O)_2$, where each $Lu^{3+}$ interacts both with carboxylate functions and neutral ether oxygen atoms of the CD scaffold. In the presence of $K^+$, the weak interaction between $Gd^{3+}$ and the neutral oxygen atoms of the CD scaffold may be disrupted to give a highly hydrated complex which induces a high relaxivity of water protons. The curve presented in Figure 6, can be seen as the signature of a binding reaction of $K^+$ to the GdACX complex existing in pure water. If this curve is fitted according to a 1:1 binding, this leads to a weak equilibrium constant $\log K \approx 2$. The interaction with $K^+$, clearly evidenced by PRE measurements, was not detected by potentiometry, suggesting that the formation constants of the $Gd^{3+}$ complexes are mainly determined by its strong electrostatic attractions with the three ACX carboxylate functions, leading to stability constants that vary little when GdACX passes from an inclusion form to a more open structure.

## 4. Conclusion

On the basis of the necessary analytical characterization of the metal complexes in solution, a rigorous framework to interpret water relaxivity has been proposed. This framework has been implemented in the case of a $Gd^{3+}$ complex with an α-CD derivative, which served as neuro-imaging contrast agent to study the vasculature of rat brain tumors[23] and has a rather complicated coordination chemistry suitable to illustrate the way to gain safe insight into the molecular factors affecting the relaxivity despite speciation pitfalls. The first NMR relaxation exploration should be a qualitative high-field PRE study to assess the additive effects of the complexes. The hydration state and the translational and rotational diffusion coefficients should then be obtained from independent techniques. Finally, longitudinal and transverse water PRE measurements at one high field complement the values of the structural and dynamic parameters governing the relaxivity of the complex at the imaging fields ≥1 T and above. To perform the previous experiments only standard equipment is required. In addition, combined NMRD and EPR studies provide the remaining parameters of the fluctuating ZFS Hamiltonian at the origin of the electronic spin relaxation effects that quench the low- and medium-field relaxivity. The proposed experimental work can be done with solutions containing about 1 mM of complex, which may avoid its problems of solubility and chemical association. The relaxivity and EPR interpretation rest on the Grenoble approach, which was recently validated[15] and provide simple SBM-like equations to interpret the medium and high-field relaxivity.

As mentioned above, at the usual imaging fields, the present case study indicates that the water relaxivity of a standard $Gd^{3+}$ complex, with its well-known IS and OS relaxation mechanisms, can be fully interpreted in terms of molecular parameters by high-field PRE measurements. The situation changes when the water dynamics with respect to $Gd^{3+}$ becomes more complicated, for instance, in the case of purely OS $Gd^{3+}$ complexes bound to serum albumine [5,72,73] and $Gd^{3+}$ ions inside hollow nanospheres[74] or nanotubes,[75] or more generally trapped inside nanoparticles.[76,77] Then, additional information obtained from a full NMRD profile and EPR spectra could be indispensable to gain reliable insight into the molecular features responsible for the relaxivity and to properly test the new required theories. The Grenoble approach can be extended to handle these systems. Indeed, this versatile simulation approach can deal with realistic models of translational, rotational, and vibrational motions involving the $Gd^{3+}$/water pair, far beyond the standard pictures of free translational and rotational diffusion that have been used until now. Furthermore, at medium and high field, the Grenoble formalism considerably simplifies because (i) relaxivity is mainly determined by the large spatial fluctuations of the dipolar magnetic field operator $\mathbf{B}_S$ that are induced by the translational and rotational $Gd^{3+}$/water random displacements and (ii) the effects of the electronic spin relaxation on relaxivity show up only through a longitudinal relaxation time due to vibrations having negligible interference with the $Gd^{3+}$/water displacements. Finally, the fact that ab initio predictions of NMRD and EPR data of $Gd^{3+}$ complexes in bulk solutions can now be envisaged thanks to recent progresses in the computation of IS hydration structure[42] and ZFS Hamiltonian[44] also supports the possibility of unravelling the various relaxivity mechanisms in more complicated systems.

**Acknowledgement.** We thank A. Moral for his experimental support, Dr. F. Genound for preliminary measurements of EPR spectra, and P.-A. Bayle for his advice on NMR spectrometers. The facilities of the Centre Grenoblois de Résonance Magnétique are acknowledged. We are indebted to Dr. M. Defranceschi for her interest in the study of lanthanide complexes in solution by NMR relaxometry and for the purchase of the Stelar relaxometer through the Nuclear Energy Division of the CEA. This research was carried out in the frame of the EC COST Action D-38 "Metal-Based Systems for Molecular Imaging Applications" and the European Molecular Imaging Laboratories (EMIL) network.

**Supporting Information Available:** The nature of electronic spin relaxation and the computation of its effects on the IS relaxivity are explained in Appendix A. The approximation of the longitudinal OS relaxivity given by eq 21 is derived in Appendix B. The theory of the EPR spectrum both in the Redfield limit and beyond is detailed in Appendix C. Figures of potentiometric titrations, $^1H$ NMR spectra of the $Lu^{3+}$ complexes, EPR spectra and $^{17}O$ NMR with $Dy^{3+}$. Tables of relaxivities and luminescence lifetimes. This material is available free of charge via the Internet at http://pubs.acs.org.

JA802347R

(72) Aime, S.; Batsanov, A. S.; Botta, M.; Howard, J. A. K.; Parker, D.; Senanayake, K.; Williams, G. *Inorg. Chem.* **1994**, *33*, 4696–4706.
(73) Caravan, P.; Greenfield, M. T.; Li, X. D.; Sherry, A. D. *Inorg. Chem.* **2001**, *40*, 6580–6587.
(74) Vasalatiy, O.; Zhao, P.; Zhang, S.; Aime, S.; Sherry, A. D. *Contrast Media Mol. Imag.* **2006**, *1*, 10–14.
(75) Sitharaman, B.; Kissell, K. R.; Hartman, K. B.; Tran, L. A.; Baikalov, A.; Rusakova, I.; Sun, Y.; Khant, H. A.; Ludtke, S. J.; Chiu, W.; Laus, S.; Toth, E.; Helm, L.; Merbach, A. E.; Wilson, L. J. *Chem. Commun.* **2005**, 3915–3917.
(76) Kim, J. S.; Rieter, W. J.; Taylor, K. M. L.; An, H.; Lin, W. L.; Lin, W. B. *J. Am. Chem. Soc.* **2007**, *129*, 8962–8963.
(77) Taylor, K. M. L.; Kim, J. S.; Rieter, W. J.; An, H.; Lin, W. L.; Lin, W. B. *J. Am. Chem. Soc.* **2008**, *130*, 2154–2155.